Biochemistry and Biophysics Reports 35 (2023) 101505

Contents lists available at ScienceDirect

Biochemistry and Biophysics Reports

journal homepage: www.elsevier.com/locate/bbrep

ASXL3 gene mutations inhibit cell proliferation and promote cell apoptosis in mouse cardiomyocytes by upregulating lncRNA NONMMUT063967.2

Zequn Liu [a,*,1], Yanmin Jiang [b,1], Fu Fang [a], Ru Li [a], Jin Han [a], Xin Yang [a], Qiong Deng [a], Lu-Shan Li [a], Ting-ying Lei [a], Dong-Zhi Li [a], Can Liao [a,**]

[a] Department of Prenatal Diagnostic Center, Guangzhou Women and Children's Medical Center, Guangzhou Medical University, Guangzhou, 510623, Guangdong, China
[b] Institute of Obstetrics and Gynecology, Guangzhou Women and Children's Medical Center, Guangzhou Medical University, Guangzhou, 510623, Guangdong, China

ARTICLE INFO

Keywords:
ASXL3 gene mutations
cell proliferation and apoptosis
Cardiomyocytes
lncRNA

ABSTRACT

Congenital heart disease (CHD) is a serious condition with unknown etiology. In a recent study, a compound heterozygous mutation (c.3526C > T [p.Arg1176Trp] and c.4643A > G [p.Asp1548Gly]) in the ASXL3 gene was identified, which is associated with CHD. This mutation was overexpressed in HL-1 mouse cardiomyocyte cells, leading to increased cell apoptosis and decreased cell proliferation. However, whether this effect is mediated by long noncoding RNAs (lncRNAs) is yet to be determined. We identified the differences among lncRNA and mRNA profiles in mouse heart tissues using sequencing to explore this issue. We detected HL-1 cell proliferation and apoptosis through CCK8 and flow cytometry. Fgfr2, lncRNA, and Ras/ERK signaling pathway expressions were evaluated using quantitative real time polymerase chain reaction (qRT-PCR) and western blot (WB) assays. We also conducted functional investigations by silencing lncRNA NONMMUT063967.2. The sequencing revealed significant changes in lncRNA and mRNA profiles, with the expression of lncRNA NONMMUT063967.2 being significantly promoted in the ASXL3 gene mutations group (MT) while the expression of Fgfr2 being down-regulated. The *in vitro* experiments showed that ASXL3 gene mutations inhibited the proliferation of cardiomyocytes and accelerated cell apoptosis by promoting the expression of lncRNAs (NONMMUT063967.2, NONMMUT063918.2, and NONMMUT063891.2), suppressing the formation of FGFR2 transcripts, and inhibiting the Ras/ERK signaling pathway. The decrease in FGFR2 had the same effect on the Ras/ERK signaling pathway, proliferation, and apoptosis in mouse cardiomyocytes as ASXL3 mutations. Further mechanistic studies revealed that suppression of lncRNA NONMMUT063967.2 and overexpression of FGFR2 reversed the effects of the ASXL3 mutations on the Ras/ERK signaling pathway, proliferation, and apoptosis in mouse cardiomyocytes. Therefore, ASXL3 mutation decreases FGFR2 expression by upregulating lncRNA NONMMUT063967.2, inhibiting cell proliferation and promoting cell apoptosis in mouse cardiomyocytes.

1. Introduction

Congenital heart disease (CHD) is a heart structural abnormality that affects around eight out of every 1,000 live births worldwide [1]. The most prevalent related diseases are ventricular septal defects (VSDs), atrial septal defects, and tetralogy of Fallot. CHD increases the risk of heart failure, which is the leading cause of death in CHD patients and represents a severe threat to human health and a substantial socioeconomic burden [2,3]. Because the pathogenesis of CHD is unknown, there are few therapeutic options for CHD, largely surgical [4]. However, the risks of surgery are high, and complications, such as atrial fibrillation, can occur [5,6]. Therefore, it is vital to investigate the pathogenesis of CHD to manage CHD effectively.

Mutations in the additional sex combs-like 3 (ASXL3) gene have been reported to induce Bainbridge–Ropers syndrome [7], tumors [8], microcephaly, and global developmental delay [9,10]. In a recent study [11], our research team identified a compound heterozygous mutation c.3526C > T (p.Arg1176Trp) and c.4643A > G (p.Asp1548Gly) in the ASXL3 gene associated with CHD. Following overexpression in HL-1 cells, this compound heterozygous mutation increased cell apoptosis

* Corresponding author.
** Corresponding author.
E-mail addresses: perfect-qun@163.com (Z. Liu), Liuzequnyn10@163.com (C. Liao).
[1] Authorship note: Zequn Liu and Yanmin Jiang contributed equally to this work.

https://doi.org/10.1016/j.bbrep.2023.101505
Received 20 March 2023; Received in revised form 7 June 2023; Accepted 23 June 2023

and decreased cell proliferation in mouse cardiomyocytes. Additionally, it affected cardiac structure and fibrosis in mice. However, how ASXL3 mutations contribute to the pathogenesis of CHD has to be investigated.

Long noncoding RNAs (lncRNAs) are one of the largest and most diverse RNA families, with lengths larger than 200 nucleotides. Initially, it was believed that lncRNAs were by-products of RNA polymerase II transcription with no biological function. However, it has been shown that lncRNAs serve key regulatory roles in various physiological and pathological bodily processes, including systemic lupus erythematosus, cancer, multiple sclerosis, osteoarthritis, regulation of cholesterol homeostasis, and inflammatory responses, in recent years [12–17]. However, little is known about the regulatory role of lncRNAs in CHD, mainly whether lncRNAs mediate ASXL3 gene mutations that affect CHD development.

This study aimed to determine whether the ASXL3 compound heterozygous mutation regulates downstream gene expression via antisense lncRNAs, thereby participating in cardiomyocyte functional regulation.

2. Materials and methods

2.1. Cell culture

HL-1 cells were purchased from the Guangzhou Cellcook Biotech Co., Ltd. (#CC9097). The cells were cultured in Claycomb Medium (#51800C, Sigma-Aldrich, USA) with 10% fetal bovine serum (Gibco, USA), 100 μM Adrenaline (#CM1015, Cellcook), and 4 mM L-glutamine (#CM1010, Cellcook) in a cell culture incubator (37 °C, 5% CO_2). The medium was changed every 2–3 days.

2.2. Flow cytometry assay

Cell apoptosis was detected using an Annexin V-FITC/7-AAD Apoptosis Detection Kit (Sigma-Aldrich, USA). Following various treatments, HL-1 cells were digested and collected using EDTA-free trypsin and washed twice with Phosphate Buffered Saline (PBS). Then, the cells were suspended with binding buffer at 1×10^6 cells/mL, took 100 μL of cell suspension, and stained with 5 μl Annexin V-FITC and 5 μl 7-AAD for 15 min at room temperature. Finally, stained cells were analyzed by flow cytometry (FACScan, BD Biosciences).

2.3. LncRNA sequencing

Total RNA was extracted from heart samples. Ribosomal RNA was removed by hybridization digestion with an rRNA probe. Then, RNA samples were purified by polymerase chain reaction (PCR) amplification. Finally, RNA libraries were constructed. The libraries were quantified by Agilent 2100 and sequencing them with an Illumina sequencer. The sequencing data were passed through quality control and long-stranded LncRNA information analysis was performed in the presence of relevant species reference sequences or reference genomes. LncRNAs with $p < 0.05$ and ploidy alterations ≥ 1.5 were defined to be differentially expressed between the two groups.

2.4. mRNA sequencing

Total RNA was extracted from heart tissues using TRIzol reagent, and samples were sequenced using a mixture of three cardiac samples. RNA-Seq libraries were prepared using 3 μg of total RNA. The constructed libraries were evaluated for quality using an Agilent 2100 Bioanalyzer and an ABI StepOnePlus Real-Time PCR System and then sequenced using an Illumina HiSeqTM2000 (Illumina, California). Genes with $p < 0.05$ and ploidy alterations ≥ 1.5 were determined to be differentially expressed between the two groups based on the analysis of the sequencing finding raw data.

2.5. CCK8 assay

The CCK-8 kit (#abs50003-5 ml, absin) was used per the manufacturer's instructions to detect the proliferation of HL-1 cells following various treatments. Briefly, HL-1 cells were digested using Trypsin-EDTA (0.25%, #abs47047375, absin) and then plated at a density of 5×10^3 cells per well in a 96-well plate. After 24h, 48h, and 72 h, CCK-8 was added to detect the proliferation of HL-1 cells via Elx800 at 450 nm spectrophotometry.

2.6. Western blot assay

The cells were lysed in RIPA buffer with protease and phosphatase inhibitors (1:100). The BCA kit (#P0010, Beyotime) detected protein samples. Proteins were loaded on 7.5%–12% SDS-PAGE gels and then transferred to PVDF membranes (EMD Millipore, Germany). The membrane was then blocked with 5% skimmed milk in TBST buffer for 1 h at room temperature, followed by incubation with primary antibodies at 4 °C overnight (anti-Ras, #67648, 1:1000, Cell Signaling Technology; anti-ASXL3, #C6072DI210-1, 1:1000, Genscript; anti-P-ERK, #9106, 1:2000, Cell Signaling Technology; anti-FGFR2, #A12436, 1:1000, Abclonal; anti-ERK, #9102, 1:2000, Cell Signaling Technology; anti-GAPDH, #60004-1-lg, 1:10000, ProteinTech). The second antibodies were added and incubated at room temperature for 1 h. Protein bands were detected using the ECL Substrate Kit (Thermo Fisher Scientific, Massachusetts).

2.7. PCR assay

TRIzol (Invitrogen, USA) was used to extract total RNA, which was then used to create cDNA using an RNA Reverse Transcription Kit (#k1073-100, APExBIO). qPCR was conducted using ChamQ SYBR qPCR Master Mix (High ROX Premixed) (#Q341-03, Vazyme Biotech, China). The housekeeping gene used was β-actin. The $2^{(-\Delta\Delta Ct)}$ method was used to calculate the relative quantitation of mRNA expression. The sequences of primers used for qPCR are shown in Table 1.

2.8. Cell transfection

HL-1 cells were cultured in a 6-well plate. ASXL3 overexpression wild-type plasmid, compound heterozygous mutation c.3526C > T (p.Arg1176Trp), c.4643A > G (p.Asp1548Gly) plasmid, FGFR2 overexpression plasmid, and siRNA fragment against NONMMUT063967.2 and FGFR2 were designed and constructed by Sangon Biotech. According to the manufacturer's instructions, HL-1 cells were transfected with the relevant plasmids or siRNA fragments using Lipofectamine 2000 (#BL623B, Biosharp). The siRNA sequences (5′–3′) are as follows: si-NONMMUT063967.2-S: AAAAACUGUUUUAAACCGCCG; si-NONMMUT063967.2-AS: GCGGUUUAA AACAGUUUUUAA; siNC-S: UUCUCCGAACGUGUCACGUTT; siNC-AS: ACGUGACACGUUCGGAGAATT; and siFGFR2-S: GAAUGAAGACCACGA CCAAGA; siFGFR2-AS:

Table 1
Sequences of primers used for qPCR.

Gene	Primer sequence (5′-3′)
β-actin	Forward: GGCTGTATTCCCCTCCATCG; Reverse: CCAGTTGGTAACAATGCCATGT;
Fgfr2 mRNA	Forward: AATCTCCCAACCAGAAGCGT; Reverse: CCAAGTGCACCCCATCCTTA;
Fgfr2 pre-mRNA	Forward: CCGATTGTGAGCCGTAGTGA; Reverse: AAGCTTTCCAGAGGCCTAGC;
NONMMUT063891.2	Forward: TAGAAGACCAACAGCTCGGC; Reverse: AACACAGGGTGATTGCCACA;
NONMMUT063918.2	Forward: GCAGCTCACGGTTACTTCCT; Reverse: TGAAGCTTGGTGTCCTTCCG;
NONMMUT063967.2	Forward: GGTGCTTCCTCTCCATAGCC; Reverse: GCGTGGGATCCTACCTACAA;

UUGGUCGUGGUCUUCAUUCGG.

2.9. Animal model construction

As previously described [11], we generated a C57BL mouse model with ASXL3 mutation. Heart tissues were obtained from mutant (MT group) and wild-type (WT group) mice ($N = 3$) on days 14.5. All animal studies followed the guidelines from Directive 2010/63/EU of the European Parliament on protecting animals used for scientific purposes or the NIH guidelines.

2.10. Bioinformatic analysis

Six samples (three heart tissues per group, mixed samples sequenced) from the heart tissues of MT group and WT group mice at 14.5 days of life were used in this research. Removing reads with noncanonical letters or low quality and discarding the sequences shorter than 20 nt with the SOAPnuke1.4.1 software. The clean reads are then mapped to the mm9 reference genome using HISAT2. The mapped reads were counted by HTSeq v 0.6.0, and finally, the R software package edgeR was used to calculate the differentially expressed genes. There were 4,405 differential lncRNAs, of which 2,970 were upregulated in the MT group and 1,435 were downregulated in the WT group (fold change >1.5; $p < 0.05$). Besides, there were 1,675 differential mRNAs, of which 657 were upregulated in the MT group and 1,018 were downregulated in the WT group (fold change >1.5; $p < 0.05$). Homology analysis was performed by the UCSC (https://genome.ucsc.edu/index.html). The R package clusterprofiler was used for KEGG and GO analysis. The KEGG website (https://www.genome.jp/kegg/) was used for KEGG pathway analysis. GO enrichment analysis was performed on the Gene Ontology Consortium website (https://www.geneontology.org) and used to reveal the genetic regulatory networks of the differentially expressed mRNAs and lncRNAs by forming hierarchical categories based on the molecular function, biological process, and cellular component aspects.

2.11. Statistical analysis

All quantitative values were presented as mean ± standard deviation (*SD*). One-way analysis of variance was used for more than or equal to three group comparisons, two-tailed Student's *t*-test was used for two group comparisons, and Bonferroni's multiple comparison method was used for two-by-two comparisons between groups. $p < 0.05$ indicates statistically significant. The statistical software used was SPSS 22.0.

3. Results

3.1. ASXL3 mutations induce substantial alterations of lncRNA and mRNA profiles in mouse cardiac tissues

To investigate the effect of the ASXL3 gene on CHD in mice, we first constructed an ASXL3 mutant C57BL mouse model [11] and extracted cardiac tissues from mutant (MT group) and WT group) at 14.5 days of life for lncRNA sequencing (three heart tissues per group, mixed samples sequenced). The lncRNA length distribution map revealed that most

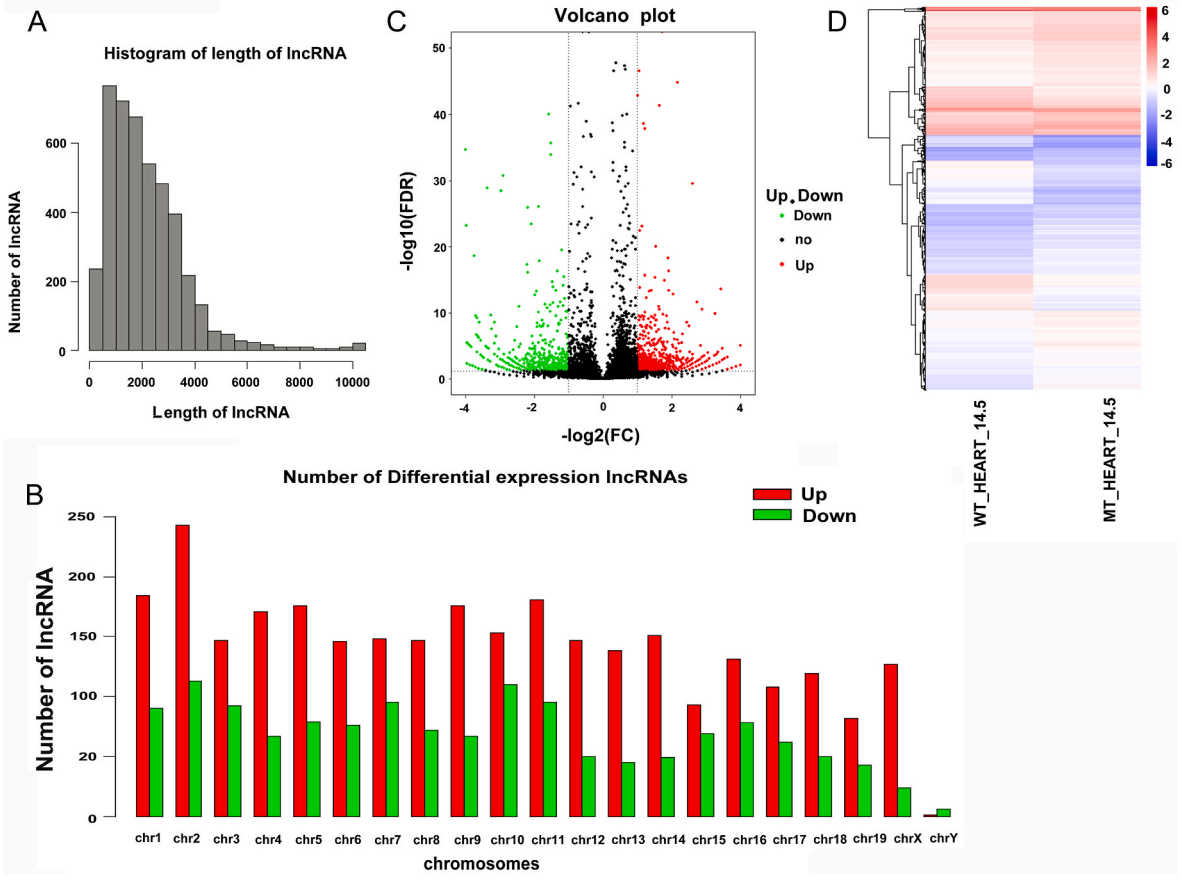

Fig. 1. The effect of ASXL3 gene mutations on the differential expression of lncRNAs in mouse cardiac tissues. (A) The length distribution of lncRNAs identified in ASXL3 gene mutation mouse heart tissue: most lncRNAs are mainly distributed between 0 and 4,000 bp. (B) The upregulated and downregulated lncRNAs were mainly distributed on chromosomes other than the Y chromosome. (C) A volcano plot illustrating the differential expression of lncRNAs in ASXL3 gene mutation mouse heart tissues. (D) Heatmap analysis of differentially expressed lncRNAs in ASXL3 gene mutation mouse cardiac tissues. Differentially expressed lncRNAs were defined by a fold change of >1.5 and a *p* value of <0.05.

lncRNAs were primarily distributed between 0 and 4,000 bp (Fig. 1A). The distribution of lncRNAs on different chromosomes showed that the upregulated and downregulated lncRNAs were mainly distributed on chromosomes other than the Y chromosome (Fig. 1B). Moreover, the volcano map (Fig. 1C) and heat map (Fig. 1D) of differential lncRNAs demonstrated that the sequencing analysis screened 4,405 differential lncRNAs, of which 2,970 were upregulated in the MT group and 1,435 were downregulated in the WT group (fold change >1.5; $p < 0.05$). These findings indicate that ASXL3 mutations induce substantial alterations of lncRNA profiles in mouse cardiac tissues.

To further investigate the changes in downstream mRNAs, mRNA sequencing analysis was performed on the cardiac tissues of mice in the MT and WT groups. mRNA distribution on different chromosomes showed that upregulated and downregulated mRNAs were mainly distributed on chromosomes other than the Y chromosome (Fig. 2A). Moreover, the differential mRNA volcano map (Fig. 2B) and heat map (Fig. 2C) demonstrated that the sequencing analysis screened 1,675 differential mRNAs, of which 657 were upregulated in the MT group and 1,018 were downregulated in the WT group (fold change >1.5; $p < 0.05$). These differentially expressed genes were also associated with various KEGG signaling pathways, including the metabolism, phosphatidylinositol 3-kinase protein kinase B (PI3K-AKT) signaling, pathways in cancer, and Rap 1 signaling pathways (Fig. 2D). These findings show that the regulatory effects of the ASXL3 gene on CHD in mice may be mediated by complex molecular mechanisms.

3.2. *ASXL3 gene mutations downregulate the expression of Fgfr2 pre-mRNA and mRNA and promote the expression of antisense lncRNAs of Fgfr2 in mouse cardiac tissues*

We then performed a clustering analysis of the differentially expressed mRNAs with the lncRNA sequencing results. We discovered that 566 lncRNAs from 329 differential mRNAs were differentially expressed (Fig. 3 and Table 2). Among them, six differentially expressed lncRNAs were derived from the Fgfr2 gene (Table 3), so these LncRNAs and Fgfr2 were identified as the next step in our study. Furthermore, qPCR experiments confirmed that the ASXL3 gene mutations decreased the expression of Fgfr2 pre-mRNA and mRNA and increased the expression of antisense lncRNAs (NONMMUT063967.2, NONMMUT063918.2, and NONMMUT063891.2) of Fgfr2 in mouse heart tissues compared with WT mice (Fig. 4). The above results suggest that the Fgfr2 gene and lncRNAs (NONMMUT063967.2, NONMMUT063918.2, and NONMMUT063891.2) mediate the regulatory effects of ASXL3 gene mutations on CHD in mice.

3.3. *ASXL3 gene mutations inhibit cell proliferation and induce cell apoptosis in mouse cardiomyocytes*

In this part of our *in vitro* investigation, we explored the effects of ASXL3 mutations on the proliferation and apoptosis of mouse cardiomyocytes. HL-1 cells were transiently transfected with the ASXL3 overexpression plasmid (WT group) and the compound heterozygous mutation plasmids c.3526C > T (p.Arg1176Trp) and c.4643A > G (p.Asp1548Gly; MT group). CCK8 assay revealed that the cell proliferation was significantly lower in the MT group at 48 h and 72 h than in the WT

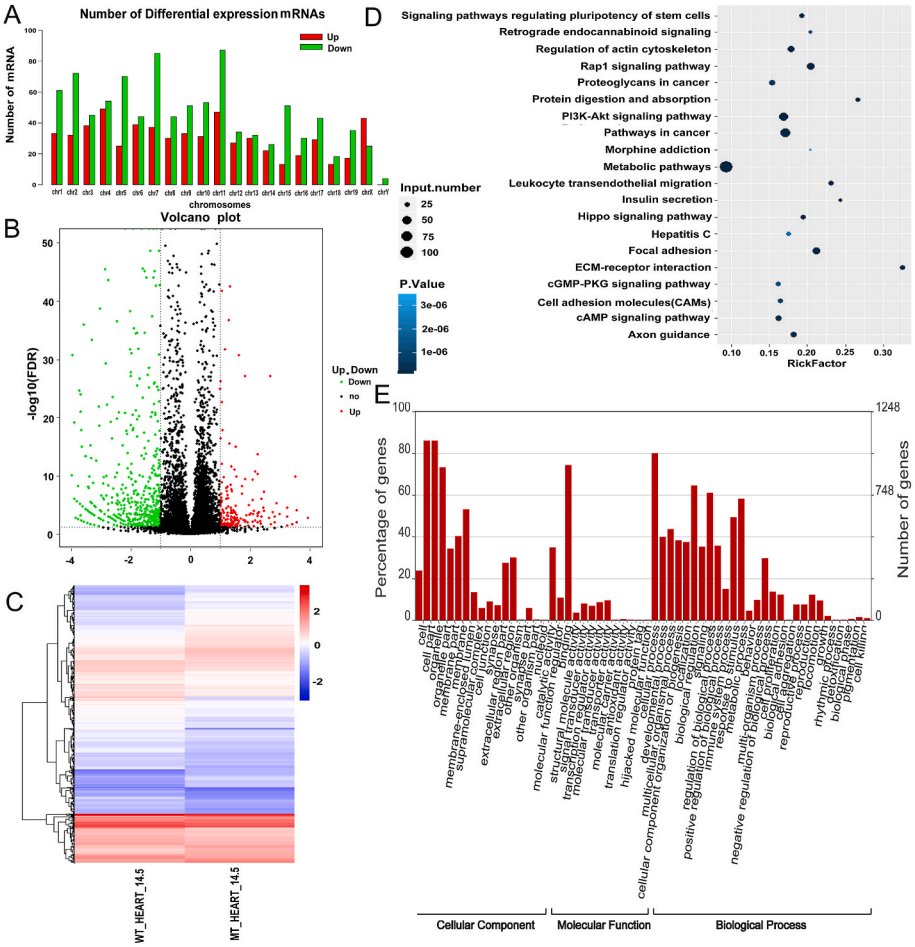

Fig. 2. The effect of ASXL3 gene mutations on the differential mRNAs expression in mouse cardiac tissues. (A) The numbers of mRNAs encoded by each mouse chromosome: the upregulated and downregulated mRNAs are mainly distributed on chromosomes other than the Y chromosome. (B) A volcano plot illustrating the differential expression of mRNAs in ASXL3 gene mutation mouse heart tissues. (C) Heatmap analysis of differentially expressed mRNAs in ASXL3 gene mutation mouse cardiac tissues. Differentially expressed mRNAs were defined by a fold change of >1.5 and a p value of <0.05. (D) KEGG enrichment analysis of differentially expressed mRNAs. (E) GO enrichment analysis of differentially expressed mRNAs.

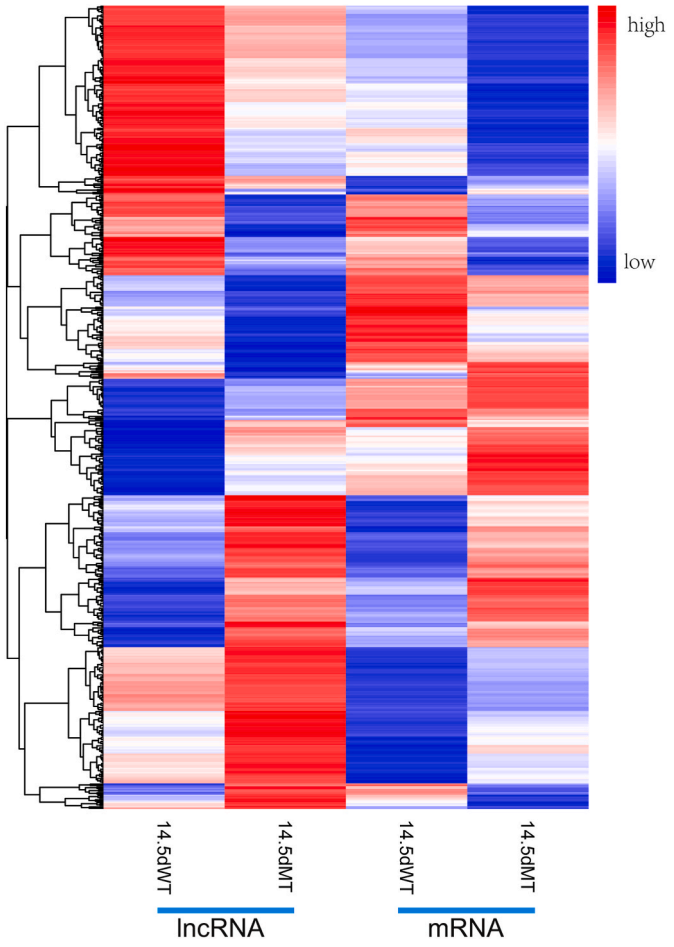

Fig. 3. Heat map of ASXL3 gene mutations on differentially encoded mRNAs and resulting differential lncRNAs clustering in heart tissues. Heat map of ASXL3 gene mutations on differentially encoded mRNAs and resulting differential lncRNAs clustering in heart tissues.

group (Fig. 5A). We then employed flow cytometry to detect apoptosis in transient HL-1 cells at 24 h and found that the number of apoptotic cells was considerably higher in the MT group than in the WT group (Fig. 5B). These results imply that the ASXL3 mutations inhibit cell proliferation and promote apoptosis in mouse cardiomyocytes.

3.4. ASXL3 compound heterozygous mutations suppress the formation of FGFR2 (NM_010207.2) transcript and the activation of the Ras/ERK signaling pathway in mouse cardiomyocytes

The ASXL3 overexpression WT plasmid group and the compound heterozygous mutation c.3526C > T (p.Arg1176Trp) and c.4643A > G (p.Asp1548Gly) plasmids (MT group) were constructed and transferred to HL-1 cells for 24 h. qPCR assay revealed no significant difference in the expression of ASXL3 between the MT and WT groups. However, the expression of FGFR2 pre-mRNA and FGFR2 mRNA was significantly downregulated, whereas the expression of NONMMUT063967.2, NONMMUT063918.2, and NONMMUT063891.2 was significantly upregulated in the MT group (Fig. 6A). The WB assay demonstrated that the expression of ASXL3 protein in the MT group was not statistically different from that of the WT group; however, the expressions of FGFR2, Ras1, and p-ERK1/2 protein were considerably downregulated (Fig. 6B). The above results indicated that the ASXL3 compound heterozygous mutation promoted the expression of lncRNAs (NONMMUT063967.2, NONMMUT063918.2, and NONMMUT063891.2), inhibited the formation of FGFR2 (NM_010207.2) transcript, and suppressed the Ras/ERK signaling pathway.

3.5. NONMMUT063967.2 inhibition reverses the effects of the ASXL3 gene mutations on FGFR2 pre-mRNA, FGFR2 mRNA, Ras/ERK signaling pathway, cell proliferation, and apoptosis in mouse cardiomyocytes

Because NONMMUT063967.2 showed the greatest differential expression fold among the three antisense lncRNAs, it was selected for further investigation. We initially constructed ASXL3 overexpression WT plasmid and compound heterozygous mutation c.3526C > T (p.Arg1176Trp) and c.4643A > G (p.Asp1548Gly) plasmid and designed and synthesized siRNA fragment against NONMMUT063967.2. HL-1 cells were transiently transfected with the ASXL3 overexpression plasmid (WT group) and the compound heterozygous mutation plasmid (MT group) and cotransfected using MT plasmid and si-NONMMUT063967.2 (MT + si-NONMMUT063967.2 group). qPCR assays revealed that interference with NONMMUT063967.2 expression reversed the ASXL3 MT-induced elevation of NONMMUT063967.2 and the downregulation of FGFR2 pre-mRNA and FGFR2 mRNA compared with the WT group (Fig. 7A). CCK8 assay showed that interfering with the expression of NONMMUT063967.2 reversed the decrease in cell proliferation induced by MT (Fig. 7B). Moreover, flow cytometry demonstrated that inhibiting the expression of NONMMUT063967.2 reversed MT's promotion of cell apoptosis (Fig. 7C). Finally, WB experiments revealed that the expression of FGFR2, Ras1, and p-ERK1/2 proteins was considerably downregulated in the MT group compared with the WT group, and interference with the expression of NONMMUT063967.2 reversed these alterations (Fig. 7D). In conclusion, the ASXL3 compound heterozygous mutations altered cardiomyocyte proliferation and apoptosis by elevating the expression of NONMMUT063967.2, consequently decreasing the formation of FGFR2 (NM_010207.2) transcripts and suppressing the Ras/ERK signaling pathway.

3.6. Knockdown of FGFR2 inhibits cell proliferation and the activation of the Ras/ERK signaling pathway while inducing cell apoptosis in mouse cardiomyocytes

To further validate the role of the downstream molecule FGFR2, we knocked down the FGFR2 in mouse cardiomyocyte HL-1 cells and found that the knockdown of the FGFR2 inhibited the proliferation of HL-1 cells (Fig. 8A). We also found that knockdown of the FGFR2 promoted cell apoptosis in HL-1 cells by flow cytometry (Fig. 8B and C). In addition, the knockdown of FGFR2 inhibited the expression of Ras1 and p-ERK1/2 (Fig. 8D), suggesting that the knockdown of FGFR2 inhibited the activation of the Ras/ERK signaling pathway. In conclusion, the knockdown of FGFR2 inhibits cell proliferation and activation of the Ras/ERK signaling pathway while inducing cell apoptosis in mouse cardiomyocytes.

3.7. Overexpression of FGFR2 reverses the effects of the ASXL3 gene mutations on Ras/ERK signaling pathway, cell proliferation, and apoptosis in mouse cardiomyocytes

The next step was to further validate the function of FGFR2 by overexpressing the FGFR2 in HL-1 cells. We found that overexpression of FGFR2 partially reversed the proliferation inhibition of HL-1 cells induced by ASXL3 gene mutations (Fig. 9A) and overexpression of FGFR2 attenuated the increase in apoptosis of HL-1 cells induced by ASXL3 gene mutations (Fig. 9B and C). In addition, WB assays of the Ras/ERK pathway showed that overexpression of FGFR2 delayed the inhibition of Ras1 and p-ERK1/2 expression induced by ASXL3 mutations (Fig. 9D), suggesting that overexpression of FGFR2 could reduce the inhibitory effect of ASXL3 mutations on the Ras/ERK signaling pathway. In conclusion, overexpression of FGFR2 reverses the effects of ASXL3 gene mutations on the Ras/ERK signaling pathway, cell

Table 2
Clustering analysis of differentially expressed mRNAs and their sources of differential lncRNAs.

LnRNA	log2 Ratio(MT/WT)	P-value	mRNA	log2 Ratio(MT/WT)	P-value
NONMMUT074721.2	2.738	9.41E-15	Mid1	2.016	1.21E-18
NONMMUT074719.2	2.619	4.05E-33	Mid1	2.016	1.21E-18
NONMMUT007679.2	2.323	1.14E-09	Hmga2	2.071	9.51E-11
NONMMUT014942.2	2.297	0.000398506	Rgs6	0.589	3.47E-05
NONMMUT146007.1	2.297	2.54E-05	Sptbn2	0.542	0.00333248
NONMMUT021903.2	2.223	0.000724352	Pcdh9	2.666	3.14E-05
NONMMUT011003.2	2.223	0.000724352	Atad5	1.537	2.72E-06
NONMMUT022736.2	2.212	4.50E-08	Prlr	2.399	2.20E-06
NONMMUT021895.2	2.204	2.12E-05	Pcdh9	2.666	3.14E-05
NONMMUT072434.2	2.121	2.50E-07	Gpc3	2.287	3.10E-186
NONMMUT032138.2	2.093	6.60E-09	Kctd16	3.160	0.01180932
NONMMUT017926.2	2.063	0.00233066	2010111I01Rik	0.634	1.13E-06
NONMMUT068453.2	1.967	1.91E-05	Ntm	1.646	0.000280726
NONMMUT069981.2	1.960	0.001810502	Prtg	5.214	8.32E-08
NONMMUT144627.1	1.960	8.72E-06	Polq	1.556	1.90E-05
NONMMUT099886.1	1.949	0.000803102	Robo1	1.804	1.25E-17
NONMMUT032963.2	1.941	0.000358758	Dcc	3.333	3.88E-10
NONMMUT062786.2	1.935	0.000161161	Tenm4	1.812	3.28E-12
NONMMUT052192.2	1.926	1.35E-16	Slit2	2.394	3.63E-60
NONMMUT074724.2	1.919	1.44E-19	Mid1	2.016	1.21E-18
NONMMUT074716.2	1.919	6.82E-06	Mid1	2.016	1.21E-18
NONMMUT139300.1	1.882	0.0071995	Lamb3	0.470	2.55E-10
NONMMUT026067.2	1.882	5.64E-05	P3h2	1.791	1.43E-05
NONMMUT070011.2	1.867	1.76E-11	Unc13c	2.370	1.75E-08
NONMMUT011679.2	1.855	1.38E-12	Igf2bp1	1.863	4.23E-33
NONMMUT074159.2	1.850	4.11E-06	Capn6	2.094	5.32E-80
NONMMUT021904.2	1.845	1.97E-05	Pcdh9	2.666	3.14E-05
NONMMUT046332.2	1.838	9.58E-05	Mmp16	1.841	0.000953372
NONMMUT108949.1	1.833	0.000212168	Garnl3	1.719	0.00264784
NONMMUT065569.2	1.804	5.13E-07	Tenm3	1.623	1.53E-07
NONMMUT112601.1	1.800	0.00540646	Chmp4c	0.652	0.01001586
NONMMUT106202.1	1.800	0.00540646	Entpd1	0.653	3.60E-07
NONMMUT041138.2	1.783	0.0124307	Eya2	0.202	1.18E-06
NONMMUT013150.2	1.783	0.0124307	Ccdc57	1.634	0.00222224
NONMMUT104442.1	1.771	1.86E-06	Kctd16	3.160	0.01180932
NONMMUT072302.2	1.771	0.000798438	Smarca1	2.032	1.24E-28
NONMMUT061972.2	1.769	1.39E-07	Igf1r	1.575	9.36E-58
NONMMUT032136.2	1.760	8.19E-13	Kctd16	3.160	0.01180932
NONMMUT018573.2	1.712	0.00918642	Vcan	2.166	6.02E-185
NONMMUT130645.1	1.712	0.00918642	Tenm3	1.623	1.53E-07
NONMMUT030933.2	1.712	0.001338776	Camkmt	0.539	0.0445508
NONMMUT021901.2	1.696	0.000450842	Pcdh9	2.666	3.14E-05
NONMMUT026390.2	1.676	0.0211758	Kalrn	1.544	2.07E-18
NONMMUT021894.2	1.676	0.0211758	Pcdh9	2.666	3.14E-05
NONMMUT072441.2	1.651	4.27E-45	Gpc3	2.287	3.10E-186
NONMMUT027219.2	1.636	1.37E-13	Robo1	1.804	1.25E-17
NONMMUT022421.2	1.629	1.91E-08	Dzip1	1.673	1.47E-05
NONMMUT074337.2	1.619	0.00497894	Wnk3	1.610	0.0230478
NONMMUT092009.1	1.578	0.000305158	Vcan	2.166	6.02E-185
NONMMUT032135.2	1.570	0.000900456	Kctd16	3.160	0.01180932
NONMMUT024117.2	1.560	0.0355382	Foxred2	0.456	0.0308878
NONMMUT014104.2	1.560	0.0355382	Nova1	1.564	0.00329086
NONMMUT016581.2	1.560	0.0355382	Zfp184	2.416	0.000144274
NONMMUT065578.2	1.551	0.000665382	Tenm3	1.623	1.53E-07
NONMMUT021930.2	1.538	0.001976656	Pcdh9	2.666	3.14E-05
NONMMUT070014.2	1.531	6.78E-12	Unc13c	2.370	1.75E-08
NONMMUT056391.2	1.531	1.95E-23	Ptn	1.715	1.10E-37
NONMMUT004581.2	1.530	3.19E-05	Mthfd1l	1.938	1.70E-09
NONMMUT039017.2	1.523	1.03E-12	Mpped2	1.720	6.26E-12
NONMMUT098308.1	1.520	0.0255088	Kalrn	1.544	2.07E-18
NONMMUT005740.2	1.520	0.0255088	Ccdc138	1.693	0.00436572
NONMMUT108702.1	1.520	0.0255088	Hacd1	0.612	5.50E-20
NONMMUT006564.2	1.520	3.98E-11	Chst11	1.586	3.64E-07
NONMMUT004930.2	1.520	0.0255088	Pde7b	1.517	0.000122305
NONMMUT130635.1	1.507	0.000268322	Tenm3	1.623	1.53E-07
NONMMUT008369.2	1.504	0.001068424	Nipsnap1	1.554	0.000587366
NONMMUT032965.2	1.499	0.00434972	Dcc	3.333	3.88E-10
NONMMUT027628.2	1.495	0.000198262	Hunk	1.673	5.16E-13
NONMMUT024424.2	1.482	0.00317792	Scube1	2.006	1.29E-07
NONMMUT024425.2	1.476	0.000108297	Scube1	2.006	1.29E-07
NONMMUT006560.2	1.444	0.001246596	Chst11	1.586	3.64E-07
NONMMUT052186.2	1.435	0.00696168	Slit2	2.394	3.63E-60
NONMMUT065571.2	1.418	5.05E-05	Tenm3	1.623	1.53E-07
NONMMUT066384.2	1.413	0.0415808	Ccdc130	1.518	0.01773832

(*continued on next page*)

Table 2 (*continued*)

LnRNA	log2 Ratio(MT/WT)	P-value	mRNA	log2 Ratio(MT/WT)	P-value
NONMMUT062718.2	1.407	0.00026641	Dlg2	2.025	3.77E-07
NONMMUT020707.2	1.405	1.64E-12	3632451O06Rik	2.069	5.90E-25
NONMMUT130651.1	1.397	0.0296478	Tenm3	1.623	1.53E-07
NONMMUT099885.1	1.397	0.0296478	Robo1	1.804	1.25E-17
NONMMUT016445.2	1.394	8.25E-06	Gli3	1.908	5.86E-13
NONMMUT062799.2	1.393	1.67E-11	Tenm4	1.812	3.28E-12
NONMMUT018471.2	1.385	5.78E-05	Polr3g	1.957	1.80E-08
NONMMUT004580.2	1.385	0.021239	Mthfd1l	1.938	1.70E-09
NONMMUT061968.2	1.385	3.35E-06	Igf1r	1.575	9.36E-58
NONMMUT032139.2	1.371	0.000413748	Kctd16	3.160	0.01180932
NONMMUT072120.2	1.371	0.000413748	Dock11	1.605	1.27E-09
NONMMUT070013.2	1.341	3.18E-08	Unc13c	2.370	1.75E-08
NONMMUT088341.1	1.339	0.001189992	Immp2l	0.513	0.0419176
NONMMUT046335.2	1.337	0.000870982	Mmp16	1.841	0.000953372
NONMMUT027013.2	1.337	0.000870982	Cmss1	0.645	0.000176958
NONMMUT059598.2	1.332	9.02E-10	Caprin2	2.171	1.07E-11
NONMMUT018576.2	1.325	4.43E-12	Vcan	2.166	6.02E-185
NONMMUT072439.2	1.324	5.46E-05	Gpc3	2.287	3.10E-186
NONMMUT005549.2	1.297	0.01723726	Grik2	4.232	1.46E-07
NONMMUT074404.2	1.297	0.000282828	Gpr173	1.684	0.00236554
NONMMUT032140.2	1.297	0.023999	Kctd16	3.160	0.01180932
NONMMUT062719.2	1.297	0.023999	Dlg2	2.025	3.77E-07
NONMMUT123798.1	1.297	0.0335506	Creb5	1.711	1.32E-15
NONMMUT098309.1	1.297	0.01723726	Kalrn	1.544	2.07E-18
NONMMUT021084.2	1.297	0.023999	Fgf9	1.556	0.000857798
NONMMUT068457.2	1.266	0.000428424	Ntm	1.646	0.000280726
NONMMUT044822.2	1.261	0.001086988	Vav3	1.521	0.000370868
NONMMUT050675.2	1.261	0.001086988	Slc25a33	0.451	0.000571126
NONMMUT026387.2	1.260	1.71E-15	Kalrn	1.544	2.07E-18
NONMMUT060084.2	1.257	1.22E-05	Hif3a	1.925	1.40E-68
NONMMUT026064.2	1.252	8.17E-11	P3h2	1.791	1.43E-05
NONMMUT045991.2	1.244	4.02E-06	Plag1	1.700	2.40E-08
NONMMUT056390.2	1.242	5.43E-06	Ptn	1.715	1.10E-37
NONMMUT070279.2	1.236	0.01379644	Lca5	1.949	4.95E-10
NONMMUT018577.2	1.231	5.72E-19	Vcan	2.166	6.02E-185
NONMMUT011680.2	1.223	0.0266258	Igf2bp1	1.863	4.23E-33
NONMMUT026719.2	1.223	0.0266258	2610015P09Rik	1.563	0.001018058
NONMMUT022617.2	1.215	0.0371958	Ptger4	0.560	0.001373816
NONMMUT000335.2	1.215	3.28E-13	Kcnq5	2.539	2.18E-10
NONMMUT143042.1	1.210	0.00420684	Wnt5a	1.836	3.11E-11
NONMMUT062775.2	1.198	0.00794684	Tenm4	1.812	3.28E-12
NONMMUT052190.2	1.197	4.61E-10	Slit2	2.394	3.63E-60
NONMMUT002690.2	1.188	2.35E-06	Kdm5b	1.538	3.66E-21
NONMMUT027220.2	1.187	5.93E-12	Robo1	1.804	1.25E-17
NONMMUT057012.2	1.187	5.93E-12	Creb5	1.711	1.32E-15
NONMMUT026065.2	1.179	0.00335306	P3h2	1.791	1.43E-05
NONMMUT000330.2	1.175	4.42E-10	Kcnq5	2.539	2.18E-10
NONMMUT046588.2	1.172	0.00459244	Bach2	1.668	8.97E-11
NONMMUT043873.2	1.165	2.58E-05	Mex3a	2.513	2.15E-70
NONMMUT123349.1	1.158	4.71E-05	Fam60a	1.738	1.82E-15
NONMMUT032957.2	1.145	0.040577	Dcc	3.333	3.88E-10
NONMMUT018578.2	1.142	1.47E-26	Vcan	2.166	6.02E-185
NONMMUT018574.2	1.129	5.85E-06	Vcan	2.166	6.02E-185
NONMMUT056435.2	1.127	0.00681388	Atp6v0a4	0.290	5.55E-05
NONMMUT010341.2	1.109	1.14E-05	Myh10	1.702	9.92E-168
NONMMUT017420.2	1.105	0.0314394	Aspn	0.650	1.56E-16
NONMMUT068681.2	1.096	2.79E-07	Gramd1b	1.695	2.79E-07
NONMMUT043874.2	1.094	4.33E-11	Mex3a	2.513	2.15E-70
NONMMUT049468.2	1.089	0.001786928	Col8a2	2.589	1.65E-09
NONMMUT029587.2	1.087	2.54E-06	Zfp57	1.560	2.72E-05
NONMMUT041533.2	1.086	0.043696	Ctcfl	2.801	2.26E-05
NONMMUT116790.1	1.086	0.043696	Zfp618	1.623	0.001527462
NONMMUT018873.2	1.086	0.00420324	Ccdc125	1.702	0.01016502
NONMMUT027223.2	1.083	0.001038534	Robo1	1.804	1.25E-17
NONMMUT046329.2	1.075	9.06E-05	Mmp16	1.841	0.000953372
NONMMUT062721.2	1.075	0.0243358	Dlg2	2.025	3.77E-07
NONMMUT021902.2	1.068	0.01372726	Pcdh9	2.666	3.14E-05
NONMMUT068679.2	1.066	0.00190616	Gramd1b	1.695	2.79E-07
NONMMUT052931.2	1.056	0.033619	Adgrl3	2.291	8.03E-08
NONMMUT022732.2	1.052	0.0188373	Prlr	2.399	2.20E-06
NONMMUT058088.2	1.044	0.00117504	Slc25a26	0.651	0.00310644
NONMMUT074055.2	1.034	0.001586812	Nrk	1.631	5.77E-41
NONMMUT032954.2	1.034	0.0145881	Dcc	3.333	3.88E-10
NONMMUT093107.1	1.034	0.0145881	Sacs	0.423	0.00056189
NONMMUT078804.1	1.022	0.00645566	Zranb3	1.797	1.11E-05
NONMMUT015327.2	1.022	0.00645566	Spata7	1.709	0.00116077

(*continued on next page*)

Table 2 (*continued*)

LnRNA	log2 Ratio(MT/WT)	P-value	mRNA	log2 Ratio(MT/WT)	P-value
NONMMUT046580.2	0.998	0.00680646	Bach2	1.668	8.97E-11
NONMMUT063321.2	0.998	0.0273542	Pde3b	1.518	1.08E-08
NONMMUT008672.2	0.985	0.021033	Cnrip1	1.740	0.01468682
NONMMUT000326.2	0.982	3.02E-07	Kcnq5	2.539	2.18E-10
NONMMUT005627.2	0.975	0.01620308	Fam184a	1.679	0.000687454
NONMMUT045472.2	0.975	0.01620308	Trmt10a	1.806	2.03E-05
NONMMUT026388.2	0.972	0.000237156	Kalrn	1.544	2.07E-18
NONMMUT056388.2	0.963	4.23E-06	Ptn	1.715	1.10E-37
NONMMUT004708.2	0.963	4.23E-06	Shprh	1.589	3.59E-11
NONMMUT066638.2	0.963	7.34E-07	Tox3	1.771	9.17E-14
NONMMUT019494.2	0.956	0.022045	4833420G17Rik	1.637	1.10E-08
NONMMUT116748.1	0.955	0.000422156	Palm2	1.755	9.21E-23
NONMMUT013151.2	0.949	0.01695564	Ccdc57	1.634	0.00222224
NONMMUT118394.1	0.949	0.01695564	Slit2	2.394	3.63E-60
NONMMUT072333.2	0.948	3.63E-06	Zfp280c	1.582	1.00E-07
NONMMUT000328.2	0.941	1.10E-06	Kcnq5	2.539	2.18E-10
NONMMUT047309.2	0.933	1.80E-08	Fsd1l	1.585	3.82E-08
NONMMUT018754.2	0.930	0.001282266	Fam169a	2.861	3.49E-17
NONMMUT051316.2	0.930	0.0230002	Hgf	3.081	0.001469944
NONMMUT032506.2	0.929	2.74E-07	Adamts19	1.527	4.04E-09
NONMMUT014324.2	0.926	2.53E-06	Mipol1	1.663	0.00309332
NONMMUT047270.2	0.925	1.34E-09	Smc2	1.535	1.90E-29
NONMMUT016834.2	0.923	2.37E-05	E2f3	1.598	3.57E-13
NONMMUT005514.2	0.922	0.01360646	Lin28b	2.172	3.44E-05
NONMMUT008957.2	0.922	0.01360646	Bcl11a	1.655	4.95E-10
NONMMUT072145.2	0.919	0.01049654	Sept6	1.713	2.59E-44
NONMMUT007326.2	0.916	1.65E-08	Osbpl8	1.522	2.33E-51
NONMMUT007327.2	0.914	1.37E-10	Osbpl8	1.522	2.33E-51
NONMMUT072143.2	0.911	5.27E-05	Sept6	1.713	2.59E-44
NONMMUT021918.2	0.910	0.040881	Pcdh9	2.666	3.14E-05
NONMMUT111697.1	0.910	0.040881	Pde4dip	0.658	7.29E-90
NONMMUT052198.2	0.909	0.00293106	Slit2	2.394	3.63E-60
NONMMUT021336.2	0.909	0.00293106	Scara3	1.708	0.000619886
NONMMUT028752.2	0.907	0.031209	Haghl	1.622	7.75E-05
NONMMUT044824.2	0.896	0.0039093	Vav3	1.521	0.000370868
NONMMUT027225.2	0.894	1.32E-05	Robo1	1.804	1.25E-17
NONMMUT000329.2	0.882	1.09E-08	Kcnq5	2.539	2.18E-10
NONMMUT026394.2	0.882	0.000261072	Kalrn	1.544	2.07E-18
NONMMUT020712.2	0.882	0.042359	3632451O06Rik	2.069	5.90E-25
NONMMUT012332.2	0.882	9.81E-05	Tanc2	1.521	1.09E-20
NONMMUT016447.2	0.876	3.82E-05	Gli3	1.908	5.86E-13
NONMMUT034047.2	0.875	0.000164924	Prune2	1.514	7.18E-07
NONMMUT050739.2	0.869	0.0053767	Errfi1	0.576	4.62E-08
NONMMUT063967.2	0.864	0.01507806	Zranb1	1.609	1.64E-12
NONMMUT063967.2	0.864	0.01507806	Fgfr2	0.560	8.28E-10
NONMMUT060116.2	0.859	0.0333578	Nova2	0.628	2.30E-06
NONMMUT046587.2	0.850	0.01196576	Bach2	1.668	8.97E-11
NONMMUT049178.2	0.843	0.00129248	Slc2a1	1.847	1.36E-52
NONMMUT026380.2	0.842	0.0262744	Kalrn	1.544	2.07E-18
NONMMUT046585.2	0.838	0.0343152	Bach2	1.668	8.97E-11
NONMMUT012359.2	0.838	0.00949572	Strada	1.577	0.0001698
NONMMUT027218.2	0.837	9.36E-05	Robo1	1.804	1.25E-17
NONMMUT061970.2	0.828	6.05E-05	Igf1r	1.575	9.36E-58
NONMMUT072833.2	0.826	0.001359284	Renbp	1.501	7.46E-05
NONMMUT022712.2	0.822	0.00084814	Skp2	1.512	7.13E-05
NONMMUT025921.2	0.813	5.38E-11	Igf2bp2	1.741	3.26E-23
NONMMUT048275.2	0.812	0.00475336	Atg4c	1.566	0.00181438
NONMMUT001367.2	0.812	0.0460866	Erbb4	1.702	2.02E-17
NONMMUT028243.2	0.807	2.70E-18	Igf2r	1.795	0
NONMMUT056852.2	0.803	3.35E-05	Igf2bp3	1.652	3.27E-21
NONMMUT019005.2	0.800	0.00300298	Nln	1.733	2.30E-12
NONMMUT026163.2	0.800	0.00300298	Tmem44	1.581	1.46E-10
NONMMUT034048.2	0.799	0.000174345	Prune2	1.514	7.18E-07
NONMMUT007332.2	0.799	3.80E-14	Osbpl8	1.522	2.33E-51
NONMMUT000331.2	0.795	3.47E-06	Kcnq5	2.539	2.18E-10
NONMMUT013443.2	0.791	0.000226656	Mycn	1.633	4.53E-07
NONMMUT008952.2	0.790	0.0282008	Bcl11a	1.655	4.95E-10
NONMMUT042114.2	0.787	0.00243594	Chmp4c	0.652	0.01001586
NONMMUT050875.2	0.786	0.000588668	Megf6	1.711	2.01E-31
NONMMUT030856.2	0.783	0.000184744	Eml4	1.626	5.79E-18
NONMMUT032970.2	0.783	0.0221258	Dcc	3.333	3.88E-10
NONMMUT011676.2	0.781	9.47E-11	Igf2bp1	1.863	4.23E-33
NONMMUT044468.2	0.780	3.24E-08	Igsf3	1.684	4.44E-33
NONMMUT074034.2	0.780	0.000375266	Fam199x	1.588	1.21E-08
NONMMUT040790.2	0.770	0.000778852	Tgif2	1.631	6.53E-10
NONMMUT139047.1	0.769	0.00661974	Erbb4	1.702	2.02E-17

(*continued on next page*)

Table 2 (*continued*)

LnRNA	log2 Ratio(MT/WT)	P-value	mRNA	log2 Ratio(MT/WT)	P-value
NONMMUT044470.2	0.769	0.00661974	Igsf3	1.684	4.44E-33
NONMMUT132327.1	0.769	0.00661974	Gramd1b	1.695	2.79E-07
NONMMUT035786.2	0.766	0.00159592	Pter	1.600	2.68E-05
NONMMUT016833.2	0.761	3.32E-06	E2f3	1.598	3.57E-13
NONMMUT030858.2	0.759	0.000401332	Eml4	1.626	5.79E-18
NONMMUT072435.2	0.753	0.01798798	Gpc3	2.287	3.10E-186
NONMMUT046583.2	0.751	0.001309502	Bach2	1.668	8.97E-11
NONMMUT001374.2	0.749	8.63E-06	Erbb4	1.702	2.02E-17
NONMMUT056857.2	0.746	0.000105595	Igf2bp3	1.652	3.27E-21
NONMMUT053621.2	0.746	0.000105595	Mtf2	1.519	3.14E-13
NONMMUT053623.2	0.738	1.14E-05	Mtf2	1.519	3.14E-13
NONMMUT143592.1	0.738	0.0386366	Ptger4	0.560	0.001373816
NONMMUT114677.1	0.734	0.0236	Runx1t1	1.608	1.15E-12
NONMMUT016444.2	0.728	0.00902346	Gli3	1.908	5.86E-13
NONMMUT012329.2	0.728	0.00902346	Tanc2	1.521	1.09E-20
NONMMUT027221.2	0.725	0.0035266	Robo1	1.804	1.25E-17
NONMMUT070015.2	0.725	0.0391506	Unc13c	2.370	1.75E-08
NONMMUT063918.2	0.724	0.0305506	Fgfr2	0.560	8.28E-10
NONMMUT000327.2	0.722	2.06E-06	Kcnq5	2.539	2.18E-10
NONMMUT149955.1	0.719	7.36E-05	Igf2bp3	1.652	3.27E-21
NONMMUT054485.2	0.715	1.56E-05	Mphosph9	1.511	4.83E-08
NONMMUT028128.2	0.712	0.0117187	Mpc1	0.533	2.96E-30
NONMMUT073706.2	0.712	0.01489186	Zfp711	1.768	6.81E-07
NONMMUT055598.2	0.710	1.02E-05	Ppp1r9a	1.612	2.99E-30
NONMMUT007328.2	0.704	6.51E-11	Osbpl8	1.522	2.33E-51
NONMMUT075131.1	0.701	0.0400292	Kcnq5	2.539	2.18E-10
NONMMUT026386.2	0.698	9.53E-07	Kalrn	1.544	2.07E-18
NONMMUT072444.2	0.698	0.0094225	Gpc3	2.287	3.10E-186
NONMMUT151395.1	0.692	2.61E-10	Cdkn1c	1.926	1.92E-117
NONMMUT004929.2	0.687	0.00597962	Pde7b	1.517	0.000122305
NONMMUT004754.2	0.685	4.46E-35	Plagl1	1.793	2.19E-186
NONMMUT035811.2	0.682	0.000962926	Hacd1	0.612	5.50E-20
NONMMUT061965.2	0.680	0.000161	Igf1r	1.575	9.36E-58
NONMMUT028244.2	0.679	6.60E-22	Igf2r	1.795	0
NONMMUT057018.2	0.678	0.000970004	Creb5	1.711	1.32E-15
NONMMUT055722.2	0.678	0.0048041	Glcci1	1.502	8.87E-08
NONMMUT057017.2	0.674	4.31E-11	Creb5	1.711	1.32E-15
NONMMUT078803.1	0.670	0.000105636	Zranb3	1.797	1.11E-05
NONMMUT029872.2	0.670	0.00194126	Trerf1	1.689	4.83E-08
NONMMUT079814.1	0.663	5.40E-23	Plagl1	1.793	2.19E-186
NONMMUT123617.1	0.663	0.00777588	Zc3hav1l	1.534	4.82E-11
NONMMUT149634.1	0.662	0.001249994	Mtf2	1.519	3.14E-13
NONMMUT007331.2	0.662	0.000509594	Osbpl8	1.522	2.33E-51
NONMMUT016449.2	0.660	0.001000736	Gli3	1.908	5.86E-13
NONMMUT046582.2	0.658	0.000801566	Bach2	1.668	8.97E-11
NONMMUT063891.2	0.656	0.0200284	Fgfr2	0.560	8.28E-10
NONMMUT015334.2	0.654	2.94E-05	Eml5	1.698	1.41E-12
NONMMUT010215.2	0.653	0.0255118	Cox10	0.660	5.58E-11
NONMMUT046579.2	0.652	0.000517426	Bach2	1.668	8.97E-11
NONMMUT039601.2	0.651	0.01253738	Slc24a5	2.370	0.00378586
NONMMUT039600.2	0.647	0.00396006	Slc24a5	2.370	0.00378586
NONMMUT056389.2	0.640	0.01264164	Ptn	1.715	1.10E-37
NONMMUT050542.2	0.635	1.19E-06	Gm13139	1.777	6.74E-14
NONMMUT063320.2	0.634	0.041804	Pde3b	1.518	1.08E-08
NONMMUT022420.2	0.633	0.01005368	Dzip1	1.673	1.47E-05
NONMMUT061964.2	0.633	5.37E-11	Igf1r	1.575	9.36E-58
NONMMUT118393.1	0.632	9.63E-07	Slit2	2.394	3.63E-60
NONMMUT004755.2	0.631	3.17E-51	Plagl1	1.793	2.19E-186
NONMMUT069593.2	0.630	0.00320046	Igdcc4	1.500	1.34E-06
NONMMUT002687.2	0.628	0.0063575	Kdm5b	1.538	3.66E-21
NONMMUT000334.2	0.620	1.70E-08	Kcnq5	2.539	2.18E-10
NONMMUT068680.2	0.619	0.0101276	Gramd1b	1.695	2.79E-07
NONMMUT001014.2	0.615	8.51E-12	Sgol2a	1.616	7.14E-18
NONMMUT015328.2	0.614	0.0204776	Spata7	1.709	0.00116077
NONMMUT015254.2	0.612	0.00640486	Flrt2	1.550	1.16E-20
NONMMUT085378.1	0.606	3.63E-06	Myh10	1.702	9.92E-168
NONMMUT027014.2	0.602	0.00034858	Cmss1	0.645	0.000176958
NONMMUT008947.2	0.601	0.0128344	Bcl11a	1.655	4.95E-10
NONMMUT068314.2	0.595	0.0330656	AB124611	2.370	0.00282878
NONMMUT132816.1	0.594	0.0205206	Zfp280d	1.557	1.23E-11
NONMMUT056993.2	0.592	0.00807632	Hibadh	0.663	4.43E-20
NONMMUT061966.2	0.592	2.16E-08	Igf1r	1.575	9.36E-58
NONMMUT045989.2	0.591	0.000676734	Plag1	1.700	2.40E-08
NONMMUT028241.2	0.590	2.08E-61	Igf2r	1.795	0
NONMMUT043871.2	0.590	0.0330514	Mex3a	2.513	2.15E-70
NONMMUT028242.2	0.585	1.19E-28	Igf2r	1.795	0

(*continued on next page*)

Table 2 (*continued*)

LnRNA	log2 Ratio(MT/WT)	P-value	mRNA	log2 Ratio(MT/WT)	P-value
NONMMUT039370.2	0.585	0.00510064	Nusap1	1.529	1.14E-18
NONMMUT034843.2	−4.245	2.13E-120	Scd1	0.108	6.16E-100
NONMMUT021476.2	−3.972	1.11E-26	Phyhip	0.189	3.65E-23
NONMMUT009017.2	−3.109	2.23E-09	Ccdc85a	0.296	4.07E-07
NONMMUT045556.2	−2.957	5.37E-32	Gbp7	0.271	7.53E-38
NONMMUT018630.2	−2.904	2.63E-34	Ckmt2	0.202	5.17E-134
NONMMUT070487.2	−2.609	5.00E-07	Paqr9	0.282	1.17E-06
NONMMUT002617.2	−2.609	5.00E-07	Cntn2	0.100	3.59E-15
NONMMUT003882.2	−2.561	1.41E-08	Mndal	0.190	5.29E-14
NONMMUT050688.2	−2.510	1.59E-05	Spsb1	0.497	2.92E-08
NONMMUT057259.2	−2.510	8.83E-11	Ndnf	0.319	1.44E-15
NONMMUT035463.2	−2.444	4.23E-14	Camk1d	0.343	4.56E-15
NONMMUT001691.2	−2.288	0.000161814	Col4a4	0.415	3.24E-08
NONMMUT040143.2	−2.253	1.08E-05	Ism1	0.186	1.81E-07
NONMMUT026407.2	−2.210	1.29E-20	Mylk	0.481	2.36E-33
NONMMUT014704.2	−2.189	1.92E-29	Akap5	0.271	6.45E-73
NONMMUT141962.1	−2.188	0.000398464	Map3k9	0.395	0.000483934
NONMMUT053385.2	−2.181	2.62E-05	Mapk10	0.349	8.11E-10
NONMMUT057260.2	−2.126	2.96E-07	Ndnf	0.319	1.44E-15
NONMMUT041793.2	−2.087	6.57E-06	Cdh4	0.469	4.08E-05
NONMMUT023954.2	−2.081	7.42E-27	Ly6e	0.348	7.70E-48
NONMMUT027008.2	−2.072	0.000304168	Cmss1	0.645	0.000176958
NONMMUT021332.2	−2.060	2.73E-09	Scara5	0.332	6.91E-12
NONMMUT035468.2	−2.060	3.12E-05	Camk1d	0.343	4.56E-15
NONMMUT053379.2	−2.048	3.52E-07	Arhgap24	0.627	8.57E-07
NONMMUT035193.2	−2.025	0.000149004	Afap1l2	0.585	0.0059685
NONMMUT045253.2	−2.025	1.55E-05	Egf	0.622	0.0280274
NONMMUT141037.1	−2.002	2.68E-07	Slfn5	0.489	2.07E-45
NONMMUT051407.2	−1.998	2.50E-06	Gsap	0.520	0.00524176
NONMMUT074764.2	−1.983	1.34E-07	Ddx3y	0.619	2.90E-21
NONMMUT034211.2	−1.971	6.18E-16	Klf9	0.283	5.98E-37
NONMMUT003506.2	−1.934	1.81E-16	Fmo2	0.449	2.33E-16
NONMMUT040873.2	−1.925	0.00109453	Snhg11	0.276	0.00081435
NONMMUT009018.2	−1.904	1.96E-11	Ccdc85a	0.296	4.07E-07
NONMMUT021458.2	−1.873	6.43E-06	Pdlim2	0.239	1.04E-11
NONMMUT026402.2	−1.867	3.12E-13	Mylk	0.481	2.36E-33
NONMMUT078902.1	−1.832	0.000382984	Ptprc	0.561	0.001118204
NONMMUT057258.2	−1.818	5.35E-11	Ndnf	0.319	1.44E-15
NONMMUT065752.2	−1.818	0.00250692	Mfap3l	0.441	1.57E-05
NONMMUT151277.1	−1.802	0.001194994	Nupr1	0.449	0.020452
NONMMUT003881.2	−1.790	2.14E-05	Mndal	0.190	5.29E-14
NONMMUT071092.2	−1.778	8.62E-11	Lrrc2	0.487	3.13E-14
NONMMUT033882.2	−1.773	0.00800142	Syt7	0.441	2.37E-15
NONMMUT078226.1	−1.767	6.51E-05	Col6a3	0.608	3.25E-43
NONMMUT116504.1	−1.761	0.00376234	Bach2	1.668	8.97E-11
NONMMUT009284.2	−1.761	0.00376234	Wwc1	0.624	0.001301556
NONMMUT032112.2	−1.742	0.000411096	Fgf1	0.573	1.55E-14
NONMMUT070486.2	−1.742	0.000411096	Paqr9	0.282	1.17E-06
NONMMUT037585.2	−1.738	6.81E-11	Kcnh7	0.407	0.00753128
NONMMUT029433.2	−1.728	1.12E-05	H2-D1	0.563	7.22E-08
NONMMUT083592.1	−1.726	5.50E-06	Irgm1	0.355	6.92E-16
NONMMUT048450.2	−1.725	2.48E-11	Ppap2b	0.543	6.29E-18
NONMMUT038723.2	−1.703	0.00126713	Lrrc4c	0.374	0.0297614
NONMMUT051274.2	−1.703	0.00561238	Pclo	0.449	0.020452
NONMMUT032720.2	−1.703	0.00265596	Ccbe1	0.279	0.000372996
NONMMUT059766.2	−1.703	0.00060838	Eps8l1	0.212	1.78E-07
NONMMUT053388.2	−1.703	0.011988	Mapk10	0.349	8.11E-10
NONMMUT063887.2	−1.703	0.00561238	Fgfr2	0.560	8.28E-10
NONMMUT064221.2	−1.703	0.00561238	Pnpla2	0.584	1.60E-14
NONMMUT031133.2	−1.703	0.011988	Nrxn1	0.269	3.52E-09
NONMMUT024689.2	−1.657	4.37E-08	Pdzrn4	0.276	5.25E-05
NONMMUT033881.2	−1.641	0.00831836	Syt7	0.441	2.37E-15
NONMMUT041791.2	−1.629	0.01782804	Cdh4	0.469	4.08E-05
NONMMUT048452.2	−1.623	5.15E-05	Ppap2b	0.543	6.29E-18
NONMMUT038063.2	−1.602	6.64E-11	Osbpl6	0.553	6.92E-05
NONMMUT026381.2	−1.596	0.00577006	Kalrn	1.544	2.07E-18
NONMMUT057892.2	−1.592	1.28E-05	Mgll	0.501	2.23E-38
NONMMUT140534.1	−1.578	9.67E-44	Lgals9	0.410	5.15E-40
NONMMUT035269.2	−1.577	0.01224468	Shtn1	0.514	0.0064129
NONMMUT050887.2	−1.577	0.01224468	Prdm16	1.589	7.55E-11
NONMMUT111696.1	−1.577	0.00031415	Pde4dip	0.658	7.29E-90
NONMMUT012551.2	−1.577	0.001916276	Abca8a	0.558	7.01E-12
NONMMUT151470.1	−1.562	6.96E-08	Ckm	0.455	0
NONMMUT017844.2	−1.554	7.96E-07	Dapk1	0.571	1.04E-18
NONMMUT024690.2	−1.551	4.57E-06	Pdzrn4	0.276	5.25E-05
NONMMUT141892.1	−1.551	0.0263018	Prpf39	1.601	8.59E-16

(*continued on next page*)

Table 2 (*continued*)

LnRNA	log2 Ratio(MT/WT)	P-value	mRNA	log2 Ratio(MT/WT)	P-value
NONMMUT068446.2	−1.548	9.97E-08	Opcml	0.563	0.00968694
NONMMUT054852.2	−1.532	2.87E-14	Upk3b	0.561	4.36E-22
NONMMUT001616.2	−1.517	2.56E-08	Epha4	0.536	4.22E-14
NONMMUT001798.2	−1.510	0.01789252	Sp100	0.145	1.69E-24
NONMMUT031138.2	−1.510	0.00580834	Nrxn1	0.269	3.52E-09
NONMMUT050578.2	−1.509	1.78E-283	Nppa	0.380	0
NONMMUT123854.1	−1.491	0.001344178	Ndnf	0.319	1.44E-15
NONMMUT040074.2	−1.491	0.001344178	Plcb1	0.618	0.00559544
NONMMUT037581.2	−1.480	0.01221964	Kcnh7	0.407	0.00753128
NONMMUT060990.2	−1.468	0.0384688	Vsig10l	1.843	0.0408746
NONMMUT069102.2	−1.468	0.0384688	Arhgap20	0.544	0.0356774
NONMMUT037344.2	−1.468	6.38E-18	Kcnj3	0.374	7.94E-30
NONMMUT013458.2	−1.468	0.0027754	Fam84a	0.411	0.000949876
NONMMUT057895.2	−1.457	0.000156546	Mgll	0.501	2.23E-38
NONMMUT060156.2	−1.453	1.10E-14	Ckm	0.455	0
NONMMUT074763.2	−1.441	3.47E-17	Uty	0.642	2.18E-06
NONMMUT012554.2	−1.440	0.025941	Abca5	1.962	4.40E-11
NONMMUT074758.2	−1.432	9.22E-09	Uty	0.642	2.18E-06
NONMMUT031121.2	−1.419	0.01759604	Nrxn1	0.269	3.52E-09
NONMMUT037584.2	−1.419	2.65E-05	Kcnh7	0.407	0.00753128
NONMMUT021777.2	−1.419	0.01759604	Rgcc	0.424	3.26E-05
NONMMUT026478.2	−1.384	1.29E-05	Slc15a2	0.372	1.79E-06
NONMMUT030928.2	−1.381	0.00563158	Prepl	0.595	2.68E-25
NONMMUT151293.1	−1.376	7.89E-143	Cox6a2	0.420	3.43E-73
NONMMUT018631.2	−1.368	2.21E-06	Ckmt2	0.202	5.17E-134
NONMMUT054765.2	−1.366	0.00267434	Ncf1	0.420	0.000257152
NONMMUT068682.2	−1.355	0.0251454	Gramd1b	1.695	2.79E-07
NONMMUT148472.1	−1.355	0.0251454	Col15a1	0.483	1.92E-51
NONMMUT002461.2	−1.335	0.000145526	Tmem163	0.468	0.000162301
NONMMUT070883.2	−1.335	0.000145526	Mapkapk3	0.510	1.62E-06
NONMMUT048755.2	−1.331	3.63E-10	Trabd2b	0.292	1.18E-56
NONMMUT034912.2	−1.313	0.000289886	Kcnip2	0.215	8.86E-87
NONMMUT127317.1	−1.312	1.46E-19	Fam174b	0.422	1.18E-53
NONMMUT023353.2	−1.293	4.11E-14	Angpt1	0.618	1.84E-17
NONMMUT048568.2	−1.288	4.65E-05	Scp2	0.660	1.14E-17
NONMMUT048568.2	−1.288	4.65E-05	Podn	0.184	9.34E-07
NONMMUT016916.2	−1.288	0.0024956	Mylk4	0.430	9.82E-09
NONMMUT015160.2	−1.288	0.0240768	Nrxn3	0.584	0.00915024
NONMMUT005849.2	−1.288	0.0052487	Tspan15	0.281	1.65E-23
NONMMUT074750.2	−1.288	3.32E-07	Eif2s3y	0.586	8.73E-12
NONMMUT011965.2	−1.270	3.14E-05	Krt222	0.409	1.24E-05
NONMMUT024692.2	−1.266	0.000187571	Pdzrn4	0.276	5.25E-05
NONMMUT130060.1	−1.260	2.42E-11	Ank1	0.620	2.39E-22
NONMMUT046264.2	−1.257	0.001654306	Runx1t1	1.608	1.15E-12
NONMMUT034209.2	−1.247	0.000125585	Klf9	0.283	5.98E-37
NONMMUT037346.2	−1.229	9.06E-15	Kcnj3	0.374	7.94E-30
NONMMUT030696.2	−1.214	6.19E-12	Eif2ak2	0.660	4.96E-14
NONMMUT014727.2	−1.212	0.0069206	Rab15	0.543	0.0030066
NONMMUT002602.2	−1.205	0.0100715	Nuak2	0.423	0.000110676
NONMMUT012550.2	−1.200	0.00216196	Abca8a	0.558	7.01E-12
NONMMUT096690.1	−1.197	0.01470112	Pdzd2	0.599	7.57E-28
NONMMUT015191.2	−1.188	0.0215352	Nrxn3	0.584	0.00915024
NONMMUT047835.2	−1.181	0.00653824	Lurap1l	0.283	3.69E-05
NONMMUT061223.2	−1.177	0.031681	Abcc8	0.469	1.29E-21
NONMMUT074760.2	−1.166	1.06E-05	Uty	0.642	2.18E-06
NONMMUT063069.2	−1.165	3.90E-07	Trim34a	0.637	0.001929562
NONMMUT052551.2	−1.162	0.00425534	Rbm47	0.321	1.31E-05
NONMMUT010754.2	−1.156	2.43E-17	Fam101b	0.648	1.16E-07
NONMMUT037345.2	−1.153	2.98E-14	Kcnj3	0.374	7.94E-30
NONMMUT020950.2	−1.138	9.46E-19	Myh6	0.222	0
NONMMUT034699.2	−1.136	0.0296012	Entpd1	0.653	3.60E-07
NONMMUT021776.2	−1.126	0.00118884	Rgcc	0.424	3.26E-05
NONMMUT044927.2	−1.118	0.000359486	Palmd	0.632	1.92E-09
NONMMUT023355.2	−1.111	2.24E-15	Angpt1	0.618	1.84E-17
NONMMUT111572.1	−1.092	0.00228536	Fdps	0.654	5.89E-07
NONMMUT017364.2	−1.086	0.00149241	Rnf144b	0.572	1.88E-05
NONMMUT014782.2	−1.085	0.00044998	Plekhh1	0.488	5.78E-09
NONMMUT018167.2	−1.081	0.0403808	Ube2ql1	0.373	0.000170558
NONMMUT023354.2	−1.078	1.24E-09	Angpt1	0.618	1.84E-17
NONMMUT018470.2	−1.072	0.0255518	Polr3g	1.957	1.80E-08
NONMMUT062142.2	−1.072	0.0255518	Rgma	0.375	7.26E-11
NONMMUT023356.2	−1.063	2.98E-13	Angpt1	0.618	1.84E-17
NONMMUT024001.2	−1.056	0.00674864	Parp10	0.492	1.90E-07
NONMMUT009826.2	−1.053	0.00437114	Slc36a2	0.453	0.01247552
NONMMUT081569.1	−1.051	2.15E-05	Fuca2	0.553	9.66E-33
NONMMUT063886.2	−1.051	0.0373026	Fgfr2	0.560	8.28E-10

(*continued on next page*)

Table 2 (*continued*)

LnRNA	log2 Ratio(MT/WT)	P-value	mRNA	log2 Ratio(MT/WT)	P-value
NONMMUT070465.2	−1.051	0.0373026	Slc9a9	1.588	0.01280208
NONMMUT072780.2	−1.035	0.001125398	Nsdhl	0.575	3.19E-05
NONMMUT057645.2	−1.029	2.46E-13	Tex261	0.585	1.63E-12
NONMMUT018229.2	−1.012	2.13E-05	Lpcat1	0.427	5.88E-13
NONMMUT065059.2	−1.011	0.00537536	Rab11fip1	0.614	0.0021823
NONMMUT057891.2	−1.007	0.000388224	Mgll	0.501	2.23E-38
NONMMUT048754.2	−1.006	2.11E-09	Trabd2b	0.292	1.18E-56
NONMMUT037583.2	−1.005	0.00090065	Kcnh7	0.407	0.00753128
NONMMUT011090.2	−1.004	0.001375562	Slfn5	0.489	2.07E-45
NONMMUT040061.2	−1.002	0.000156349	Plcb1	0.618	0.00559544
NONMMUT015187.2	−0.998	0.00497126	Nrxn3	0.584	0.00915024
NONMMUT040666.2	−0.992	1.46E-13	Trp53inp2	0.608	1.95E-108
NONMMUT023352.2	−0.990	3.99E-08	Angpt1	0.618	1.84E-17
NONMMUT030099.2	−0.988	0.01854084	Ccdc94	0.648	0.0156526
NONMMUT006953.2	−0.986	4.01E-17	Socs2	0.395	1.92E-51
NONMMUT006741.2	−0.979	7.65E-05	Chpt1	0.544	5.60E-23
NONMMUT052907.2	−0.978	0.01096684	Adgrl3	2.291	8.03E-08
NONMMUT066150.2	−0.978	1.71E-15	Tmem38a	0.594	4.13E-34
NONMMUT072401.2	−0.976	0.045926	Stk26	2.049	1.11E-08
NONMMUT020946.2	−0.970	2.76E-09	Myh6	0.222	0
NONMMUT009737.2	−0.967	1.14E-22	Uqcrq	0.591	1.32E-49
NONMMUT048453.2	−0.963	1.79E-07	Ppap2b	0.543	6.29E-18
NONMMUT011091.2	−0.956	3.45E-05	Slfn5	0.489	2.07E-45
NONMMUT045415.2	−0.956	0.0420284	Slc39a8	0.492	9.22E-14
NONMMUT045100.2	−0.953	0.0021716	Pde5a	0.554	3.62E-11
NONMMUT039400.2	−0.948	5.26E-45	Ehd4	0.527	4.58E-125
NONMMUT014781.2	−0.944	6.65E-07	Plekhh1	0.488	5.78E-09
NONMMUT013651.2	−0.940	0.038432	Taf1b	1.669	1.51E-05
NONMMUT037577.2	−0.940	0.038432	Kcnh7	0.407	0.00753128
NONMMUT145793.1	−0.933	3.91E-16	Prdx5	0.611	3.64E-30
NONMMUT066308.2	−0.932	0.00281934	Inpp4b	0.661	6.49E-08
NONMMUT048451.2	−0.931	0.001028806	Ppap2b	0.543	6.29E-18
NONMMUT051066.2	−0.929	3.54E-11	Perm1	0.450	2.43E-45
NONMMUT000717.2	−0.927	7.52E-27	Tmem182	0.577	1.31E-15
NONMMUT057893.2	−0.925	0.001565884	Mgll	0.501	2.23E-38
NONMMUT141090.1	−0.925	5.69E-08	Cisd3	0.576	2.09E-06
NONMMUT030927.2	−0.914	3.14E-06	Prepl	0.595	2.68E-25
NONMMUT007234.2	−0.912	0.0320856	Lin7a	0.539	0.00891776
NONMMUT038061.2	−0.912	0.0320856	Osbpl6	0.553	6.92E-05
NONMMUT021924.2	−0.897	0.000351624	Pcdh9	2.666	3.14E-05
NONMMUT019197.2	−0.895	0.00512152	Zswim6	1.502	3.55E-05
NONMMUT066304.2	−0.890	0.0267536	Inpp4b	0.661	6.49E-08
NONMMUT023358.2	−0.888	0.000167523	Angpt1	0.618	1.84E-17
NONMMUT056384.2	−0.882	2.71E-12	Chrm2	0.453	8.69E-16
NONMMUT153091.1	−0.881	0.0244232	Cep57	1.612	1.29E-12
NONMMUT147464.1	−0.861	5.35E-33	S100a1	0.538	1.52E-31
NONMMUT052614.2	−0.860	0.0100808	Atp8a1	0.439	2.00E-28
NONMMUT006742.2	−0.858	5.16E-09	Chpt1	0.544	5.60E-23
NONMMUT027011.2	−0.857	0.000229096	Cmss1	0.645	0.000176958
NONMMUT030929.2	−0.857	0.0050558	Prepl	0.595	2.68E-25
NONMMUT030929.2	−0.857	0.0050558	Camkmt	0.539	0.0445508
NONMMUT063240.2	−0.855	0.00921798	Galnt18	0.527	2.78E-09
NONMMUT041297.2	−0.848	0.000613284	Tmem189	0.664	1.54E-06
NONMMUT037582.2	−0.847	0.0315402	Kcnh7	0.407	0.00753128
NONMMUT052391.2	−0.843	0.001969692	Arap2	0.576	0.000134713
NONMMUT020163.2	−0.843	0.00051656	Lrtm1	0.517	2.55E-08
NONMMUT065898.2	−0.838	3.14E-07	Lpl	0.611	1.73E-185
NONMMUT068322.2	−0.836	0.00644372	Tmem205	0.636	0.01439384
NONMMUT015186.2	−0.830	0.01176984	Nrxn3	0.584	0.00915024
NONMMUT151258.1	−0.830	8.74E-35	Ndufab1	0.660	1.63E-18
NONMMUT015171.2	−0.823	0.0216958	Nrxn3	0.584	0.00915024
NONMMUT022803.2	−0.821	0.00209206	Pdzd2	0.599	7.57E-28
NONMMUT003137.2	−0.820	6.71E-07	Fam129a	0.636	1.22E-10
NONMMUT066307.2	−0.818	0.001915408	Inpp4b	0.661	6.49E-08
NONMMUT120553.1	−0.812	0.0404926	Arap2	0.576	0.000134713
NONMMUT046610.2	−0.812	0.0404926	Ankrd6	1.784	9.67E-06
NONMMUT005420.2	−0.808	0.00682366	Lace1	0.652	1.64E-05
NONMMUT047476.2	−0.807	0.0367836	Dnajc25	0.645	0.001381516
NONMMUT147521.1	−0.802	0.0334252	Trmt13	1.574	0.00715314
NONMMUT070469.2	−0.802	0.0334252	Slc9a9	1.588	0.01280208
NONMMUT107817.1	−0.801	6.64E-06	Ehd4	0.527	4.58E-125
NONMMUT046621.2	−0.797	0.000793952	Pm20d2	0.613	2.08E-06
NONMMUT034698.2	−0.787	0.00860934	Entpd1	0.653	3.60E-07
NONMMUT020944.2	−0.764	8.80E-70	Myh6	0.222	0
NONMMUT005623.2	−0.759	0.0288672	Mcm9	1.703	1.62E-06
NONMMUT019496.2	−0.750	0.00360454	4833420G17Rik	1.637	1.10E-08

(*continued on next page*)

Table 2 (*continued*)

LnRNA	log2 Ratio(MT/WT)	P-value	mRNA	log2 Ratio(MT/WT)	P-value
NONMMUT000571.2	−0.749	3.27E-05	Ankrd23	0.494	6.18E-20
NONMMUT016357.2	−0.749	4.00E-34	Ryr2	0.603	1.09E-291
NONMMUT034702.2	−0.747	0.01487496	Entpd1	0.653	3.60E-07
NONMMUT041003.2	−0.740	2.61E-05	Fitm2	0.627	0.000112943
NONMMUT009622.2	−0.736	0.000599938	Adamts2	0.610	1.93E-12
NONMMUT001369.2	−0.735	0.0486344	Erbb4	1.702	2.02E-17
NONMMUT035466.2	−0.734	0.000459816	Camk1d	0.343	4.56E-15
NONMMUT139656.1	−0.729	0.0298984	Socs2	0.395	1.92E-51
NONMMUT110012.1	−0.721	0.00878514	Trp53inp2	0.608	1.95E-108
NONMMUT044223.2	−0.719	0.00666032	Car14	0.528	3.46E-16
NONMMUT015981.2	−0.718	2.33E-10	Ckb	0.558	2.55E-52
NONMMUT095269.1	−0.703	6.90E-06	Pdzd2	0.599	7.57E-28
NONMMUT027012.2	−0.703	0.00209424	Cmss1	0.645	0.000176958
NONMMUT063943.2	−0.703	0.0411164	Fgfr2	0.560	8.28E-10
NONMMUT020947.2	−0.697	2.56E-102	Myh6	0.222	0
NONMMUT027010.2	−0.695	7.63E-08	Cmss1	0.645	0.000176958
NONMMUT018241.2	−0.684	0.01470708	Cep72	1.550	0.001564074
NONMMUT063503.2	−0.674	2.57E-07	Ndufab1	0.660	1.63E-18
NONMMUT056385.2	−0.671	4.66E-16	Chrm2	0.453	8.69E-16
NONMMUT022958.2	−0.655	0.0387152	Ank	0.640	9.61E-09
NONMMUT002318.2	−0.654	0.0426538	Tfcp2l1	0.639	0.0023675
NONMMUT043560.2	−0.653	4.96E-06	Rxfp1	0.637	6.03E-06
NONMMUT043997.2	−0.653	0.00425696	Adar	0.637	9.59E-12
NONMMUT016363.2	−0.649	3.49E-11	Ryr2	0.603	1.09E-291
NONMMUT005454.2	−0.649	0.01832358	Pdss2	0.589	8.62E-05
NONMMUT051210.2	−0.647	0.0201272	Tmem243	0.478	0.00206092
NONMMUT040063.2	−0.646	0.0221142	Plcb1	0.618	0.00559544
NONMMUT011457.2	−0.645	0.00883088	Trim25	0.627	1.29E-14
NONMMUT033200.2	−0.637	2.70E-11	Pqlc1	0.639	1.30E-08
NONMMUT104363.1	−0.635	0.0391514	Pcdhga2	2.550	4.00E-06
NONMMUT043292.2	−0.634	0.01852034	Arhgef26	0.618	0.000780098
NONMMUT074713.2	−0.621	2.09E-05	Mid1	2.016	1.21E-18
NONMMUT006035.2	−0.619	0.01079788	Rtkn2	0.560	1.71E-05
NONMMUT154169.1	−0.618	0.0033763	Ebp	0.636	0.000508062
NONMMUT016361.2	−0.603	5.74E-15	Ryr2	0.603	1.09E-291
NONMMUT060031.2	−0.593	4.55E-21	Ehd2	0.655	1.25E-39

Table 3
Gene information for six differentially expressed LncRNAs that are generated from Fgfr2.

geneID	log2 Ratio(MT/WT)	Up-Down-Regulation (MT/WT)	P-value	Strand
NONMMUT063967.2	0.864449168	Up	0.01507806	–
NONMMUT063918.2	0.72367333	Up	0.0305506	–
NONMMUT063891.2	0.656489668	Up	0.0200284	–
NONMMUT063887.2	−1.702591425	Down	0.00561238	+
NONMMUT063886.2	−1.050514728	Down	0.0373026	–
NONMMUT063943.2	−0.702591425	Down	0.0411164	–

proliferation, and apoptosis in mouse cardiomyocytes.

4. Discussion

In this study, sequencing of cardiac tissues from C57BL mice with ASXL3 mutations revealed significant alterations in the lncRNA and mRNA profiles. Expression of lncRNA NONMMUT063967.2 was considerably increased in the MT group, but the expression of Fgfr2 was decreased. In *in vitro* experiments, ASXL3 gene mutations inhibited cardiomyocyte proliferation and accelerated apoptosis by suppressing the formation of FGFR2 transcripts and blocking the Ras/ERK signaling pathway. The decrease in FGFR2 had the same effect on the Ras/ERK signaling pathway, proliferation, and apoptosis in mouse cardiomyocytes as ASXL3 mutations. Further mechanistic studies revealed that both suppression of the lncRNA NONMMUT063967.2 and overexpression of FGFR2 reversed the effects of the ASXL3 mutations on the Ras/ERK signaling pathway, proliferation, and apoptosis in mouse cardiomyocytes. In conclusion, the ASXL3 mutations decreased FGFR2

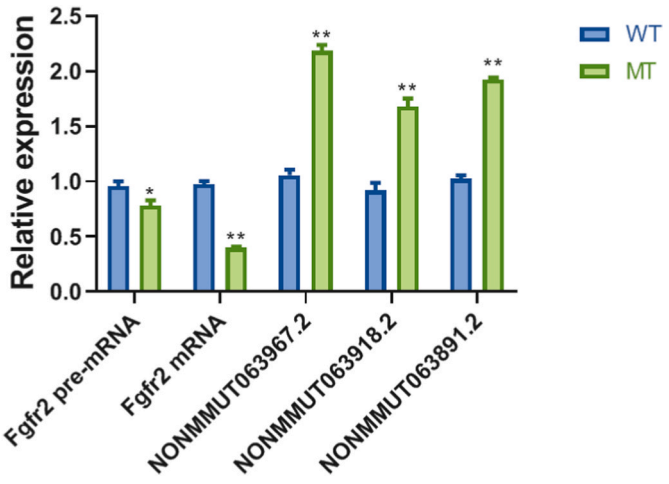

Fig. 4. The effect of ASXL3 gene mutation on the expression of Fgfr2 pre-mRNA, mRNA, and antisense lncRNAs of Fgfr2 in mouse heart tissues. Relative RNA expression of Fgfr2 pre-mRNA, Fgfr2 mRNA (NM_010207.2), and lncRNAs (NONMMUT063967.2, NONMMUT063918.2, and NONMMUT063891.2) in WT and MT groups. *$p < 0.05$, **$p < 0.01$.

expression by upregulating lncRNA NONMMUT063967.2, ultimately inhibiting the cell proliferation of mouse cardiomyocytes and promoting cell apoptosis.

Our previous study [11] revealed mutations in the ASXL3 gene, c.3526C > T (p.Arg1176Trp), and c.4643A > G (p.Asp1548Gly), which are related to CHD. Following overexpression in HL-1 cells, these compound heterozygous mutations increased cell apoptosis and decreased cell proliferation in cardiomyocytes. In addition, it impacted the

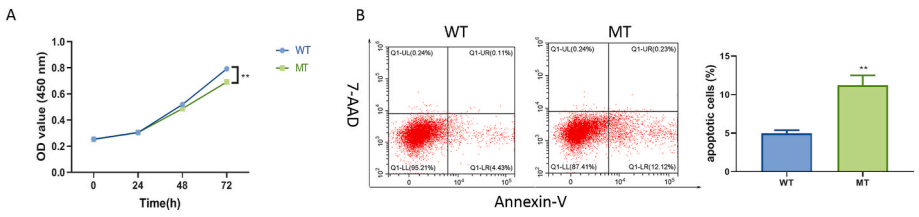

Fig. 5. The effect of ASXL3 gene mutation on proliferation and apoptosis in mouse cardiomyocytes. ASXL3 overexpression plasmid (WT group) and compound heterozygous mutation c.3526C > T (p.Arg1176Trp) and c.4643A > G (p.Asp1548Gly) plasmids (MT group) were constructed and transiently transferred to HL-1 cells. (A) CCK8 assay detected cell proliferation at 0, 24, 48, and 72 h of transfection. (B) Apoptosis was detected in both groups of cells using flow cytometry at 24 h of transfection. $^{**}p < 0.01$.

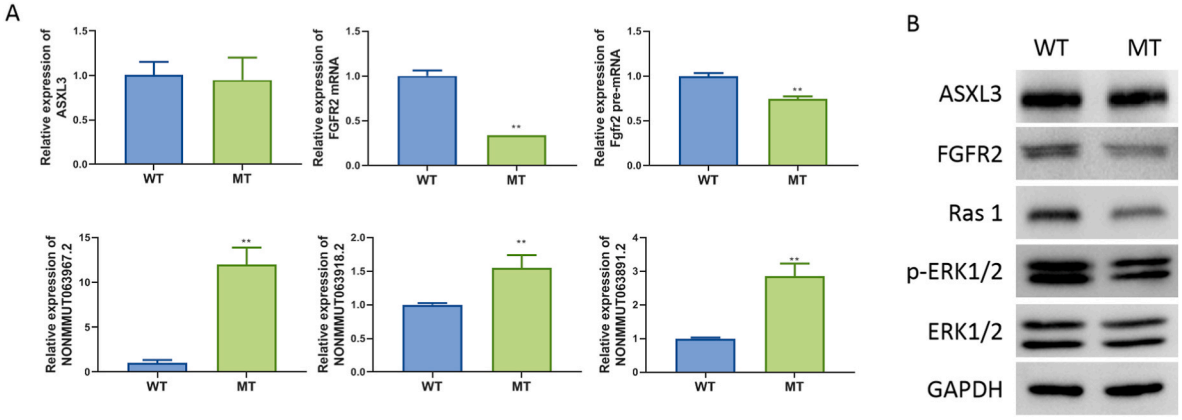

Fig. 6. Effect of ASXL3 gene mutation on Fgfr2 pre-mRNA, mRNA, and antisense lncRNA expression of Fgfr2 and the Ras/ERK signaling pathway in mouse cardiomyocytes. The ASXL3 overexpression wild-type plasmid (WT group) and the compound heterozygous mutation c.3526C > T (p.Arg1176Trp) and c.4643A > G (p.Asp1548Gly) plasmids (MT group) were constructed. (A) The gene expression of ASXL3, FGFR2 mRNA (NM_010207.2), NONMMUT063967.2, NONMMUT063918.2, and NONMMUT063891.2 were detected by qPCR in transiently transfected HL-1 cells at 24 h. (B) After 48 h of transient rotation, each group of proteins was collected for WB assays to identify the protein expression of ASXL3, FGFR2, Ras 1, p-ERK1/2, and ERK1/2. $^{*}p < 0.05$, $^{**}p < 0.01$.

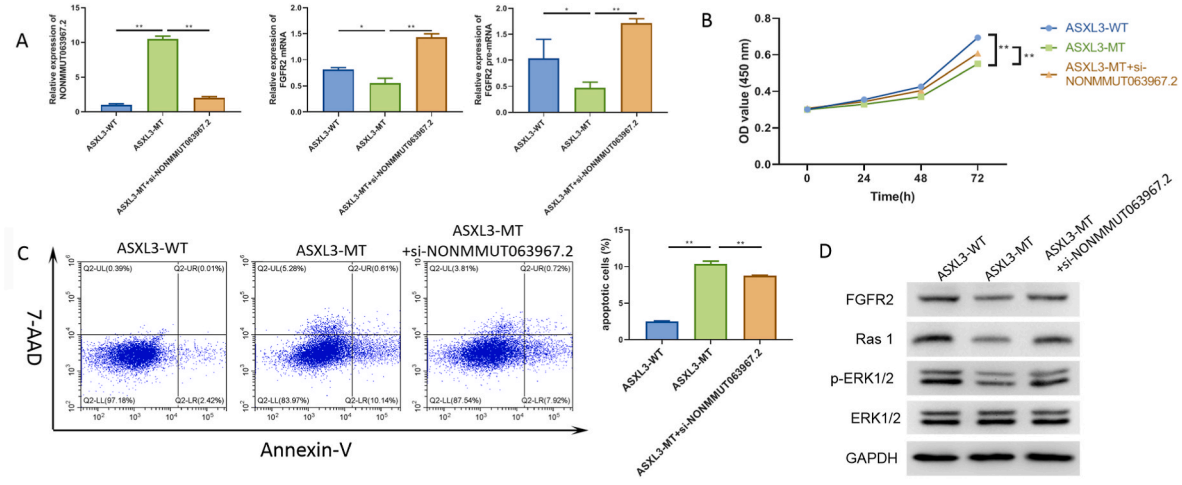

Fig. 7. Inhibition of NONMMUT063967.2 reverses the effect of the ASXL3 gene mutation on FGFR2 pre-mRNA, FGFR2 mRNA, Ras/ERK signaling pathway, and apoptosis in mouse cardiomyocytes. ASXL3 overexpression plasmid and compound heterozygous mutation c.3526C > T (p.Arg1176Trp) and c.4643A > G (p.Asp1548Gly) plasmids were constructed, and siRNA fragments targeting NONMMUT063967.2 were designed and synthesized. HL-1 cells were transiently transfected with the ASXL3 overexpression plasmid (WT group) and compound heterozygous mutation plasmid (MT group) and cotransfected using MT plasmid and si-NONMMUT063967.2 (MT + si-NONMMUT063967.2 group). (A) Gene expression NONMMUT063967.2, ASXL3, and FGFR2 mRNA (NM_010207.2) was detected by qPCR 24 h after the transient transfer of HL-1 cells. (B) Cell activity at 0 h, 24 h, 48 h, and 72 h was measured by the CCK8 assay. (C) Detecting cell apoptosis using flow cytometry after a 24 h transient. (D) FGFR2, Ras 1, p-ERK1/2, and ERK1/2 protein expression were evaluated using WB assays after 48 h of transient rotation. $^{*}p < 0.05$, $^{**}p < 0.01$.

structure and fibrosis of the mouse heart. However, it remains unclear how ASXL3 gene mutations contribute to the pathogenesis of CHD. In the present study, we discovered that ASXL3 mutations suppressed FGFR2 expression through the upregulation of lncRNA NONMMUT063967.2, thereby suppressing cardiomyocyte proliferation and promoting cell apoptosis.

Our present study discovered that Fgfr2 expression was suppressed in the cardiac tissue of ASXL3-mutant C57BL mice. *In vitro* experiments further reveal that ASXL3 mutations inhibit cardiomyocyte proliferation and promote apoptosis by suppressing the formation of FGFR2

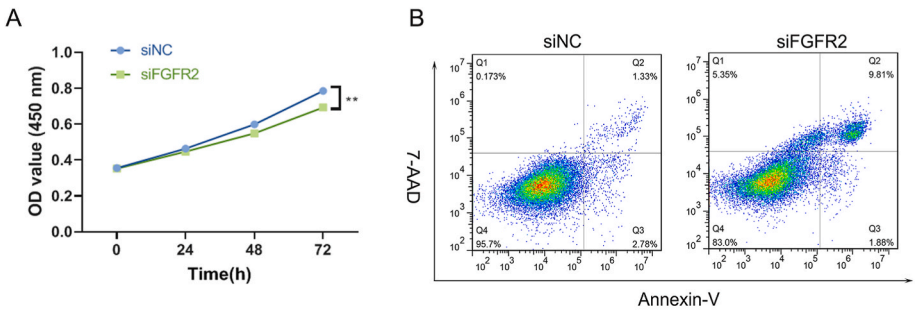

Fig. 8. Effect of FGFR2 knockdown on cell proliferation, cell apoptosis, and Ras/ERK signaling in mouse cardiomyocytes. (A) Cell activity in siNC and siFGFR2 groups at 0 h, 24 h, 48 h, and 72 h was measured by CCK8 assay. (B) Detection of cell apoptosis by flow cytometry after the 24 h transient. (C) Quantitative results of apoptotic cells as determined by flow cytometry in (B). (D) After 48-h transient rotation, each protein group was collected for WB assays to identify the protein expression of FGFR2, Ras 1, p-ERK1/2, and ERK1/2. $^{**}p < 0.01$.

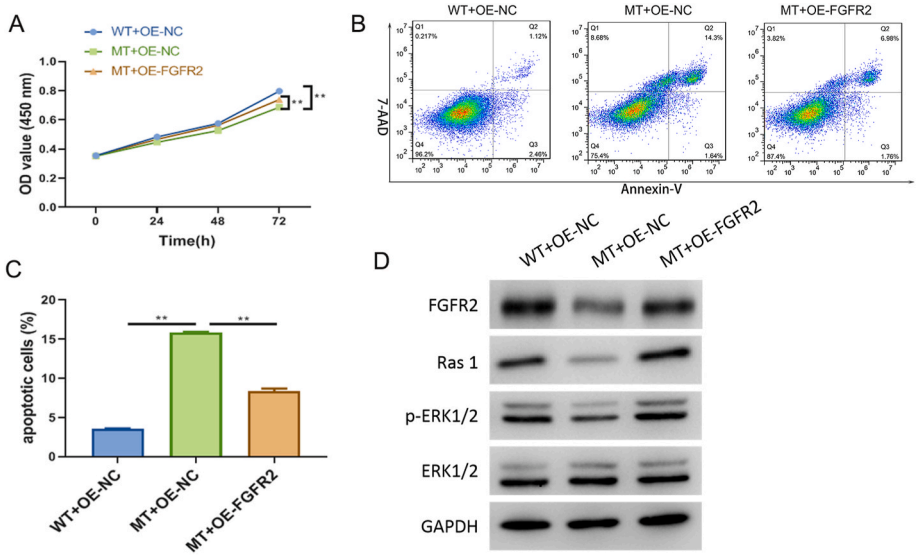

Fig. 9. Overexpression of FGFR2 reverses the effects of ASXL3 gene mutations on Ras/ERK signaling, cell proliferation, and apoptosis in mouse cardiomyocytes. (A) Cell activity in different groups at 0 h, 24 h, 48 h, and 72 h was measured by the CCK8 assay. (B) Detection of cell apoptosis by flow cytometry after the 24 h transient. (C) Quantitative results of apoptotic cells as determined by flow cytometry in (B). (D) After 48 h transient rotation, each protein group was collected for WB assays to identify the protein expression of FGFR2, Ras 1, p-ERK1/2, and ERK1/2. $^{**}p < 0.01$.

transcripts. Besides, the knockdown of FGFR2 can mimic the effects of the mutated ASXL3, and overexpression of FGFR2 reverses the effects of the ASXL3 gene mutations on Ras/ERK signaling pathway, cell proliferation, and apoptosis in mouse cardiomyocytes, which is strong evidence that Fgfr2 plays an important regulatory role in ASXL3 mutations affecting mouse cardiac function. Several prior studies have also demonstrated that Fgfr2 regulates heart disease. Marguerie et al. [18] discovered that the major cardiac defect in Fgfr2-IIIb mutant mouse embryos was a VSD; a fraction of the mice also had cardiac outflow tract and right ventricular dysplasia. Moreover, deletion of Fgfr2-IIIb was associated with ventricular abnormalities, including thin myocardial walls, abnormal trabeculae, and muscular VSDs. Huang et al. [19] found that FGFR2 regulates murine cardiac fibroblasts' activation, proliferation, and migration via miR-338-3p. Furthermore, mutations in p. Ser252Trp and p.Pro253Arg of the FGFR2 gene led to Abbott syndrome associated with the development of CHD [20]. In conclusion, Fgfr2 plays a crucial regulatory role in cardiac disease.

LncRNAs play a key regulatory role in heart disorders and various diseases. There are several ways in which lncRNAs exert their inhibitory effects, most commonly by directly regulating the function of mRNAs or by regulating the expression of miRNAs, thereby affecting the expression of target genes [21,22]. In this research, the lncRNA NONMMUT063967.2 may function by regulating the gene expression of Fgfr2. In this research, the lncRNA NONMMUT063967.2 may function by regulating the gene expression of Fgfr2. In this study, we found that lncRNAs (NONMMUT063967.2, NONMMUT063918.2, and NONMMUT063891.2) were increased in the heart tissues of C57BL mice with ASXL3 mutations. *In vitro* experiments also showed that ASXL3 mutations inhibited cardiomyocyte proliferation and promoted cell apoptosis by promoting the expression of lncRNAs (NONMMUT063967.2, NONMMUT063918.2, and NONMMUT063891.2). In addition, suppression of lncRNA NONMMUT063967.2 restored the effects of the ASXL3 mutation

on FGFR2 expression, the Ras/ERK signaling pathway, cell proliferation, and apoptosis in mouse cardiomyocytes. This shows that lncRNAs play a crucial role in regulating mouse cardiac function by ASXL3 mutations. Additionally, previous research has demonstrated that lncRNA molecules regulate heart disorders [23–25]. Ma et al. [26] discovered that lncRNA SAP30–2:1 was downregulated in CHD and could regulate cell proliferation by targeting HAND2. Lu et al. [27] found that lncRNA SNHG14 attenuated hypoxia-induced damage to rat ventricular cardiomyocytes H9c2 cells by targeting the miR-25-3p/KLF4 axis. Furthermore, Zhu et al. [28] discovered that lncRNA TUG1 targets miR-29c during chronic hypoxia to promote the conversion of cardiac fibroblasts to myofibroblasts, hence exacerbating the chronic hypoxia-induced deterioration of fibrosis. Above all, these studies indicate that lncRNAs play an important regulatory function in cardiac diseases.

There are several limitations to this study. First, this study lacks *in vivo* functional validation experiments on lncRNA NONMMUT063967.2 in animals. Second, the mechanistic investigations in this study focused primarily on the mediating role of lncRNA NONMMUT063967.2 and lacked validation for two other lncRNA molecules (NONMMUT063918.2 and NONMMUT063891.2). Third, there is no important validation of clinical samples in this study. Lastly, this study failed to validate the regulation between lncRNA NONMMUT063967.2 and the Fgfr2 gene, which is a future research direction for our group.

5. Conclusion

ASXL3 gene mutations inhibit FGFR2 expression through upregulation of lncRNA NONMMUT063967.2, thus inhibiting cell proliferation of mouse cardiomyocytes and promoting cell apoptosis.

Funding

This study was supported by the Research Foundation of Guangzhou Women and Children's Medical Center for Clinical Doctor and the clinical doctor of Guangzhou Women and Children's Medical center/Guangzhou Institute of Pediatrics (YIP-2019-020 and YIP-2019-030), the National Natural Science Foundation of China (81901491), and Guangzhou Science and Technology Plan Project (202201010420240049).

Access to information and materials

The datasets analyzed during the research are available upon reasonable request from the corresponding author.

Declaration of competing interest

The authors declare that they have no known competing financial interests or personal relationships that could have appeared to influence the work reported in this paper.

References

[1] D. van der Linde, E.E. Konings, M.A. Slager, M. Witsenburg, W.A. Helbing, J. J. Takkenberg, J.W. Roos-Hesselink, Birth prevalence of congenital heart disease worldwide: a systematic review and meta-analysis, J. Am. Coll. Cardiol. 58 (21) (2011) 2241–2247, https://doi.org/10.1016/j.jacc.2011.08.025.

[2] M. Brida, D. Lovrić, M. Griselli, F. Riesgo Gil, M.A. Gatzoulis, Heart failure in adults with congenital heart disease, Int. J. Cardiol. 357 (2022) 39–45, https://doi.org/10.1016/j.ijcard.2022.03.018.

[3] C.W. Lu, J.K. Wang, H.L. Yang, A.H. Kovacs, K. Luyckx, F.J. Ruperti-Repilado, A.V. D. Bruaene, J. Enomoto, M.A. Sluman, J.L. Jackson, P. Khairy, S.C. Cook, S. Chidambarathanu, L. Alday, E. Oechslin, K. Eriksen, M. Dellborg, M. Berghammer, B. Johansson, A.S. Mackie, S. Menahem, M. Caruana, G. Veldtman, A. Soufi, S.M. Fernandes, K. White, E. Callus, S. Kutty, S. Apers, P. Moons, Heart failure and patient-reported outcomes in adults with congenital heart disease from 15 countries, J. Am. Heart Assoc. 11 (9) (2022), e024993, https://doi.org/10.1161/jaha.121.024993.

[4] B.J. Farr, M. Castillo-Angeles, B. Okafor, N. Patel, R. Ramsis, N. Aldweib, A. R. Opotowsky, D. Nehra, S.E. Rice-Townsend, Adult survivors of moderate and great complexity congenital heart disease undergoing general surgery procedures: how do they fare? Am. J. Surg. 223 (5) (2022) 841–845, https://doi.org/10.1016/j.amjsurg.2021.08.021.

[5] C.R. Parikh, J.H. Greenberg, E. McArthur, H. Thiessen-Philbrook, A.D. Everett, R. Wald, M. Zappitelli, R. Chanchlani, A.X. Garg, Incidence of ESKD and mortality among children with congenital heart disease after cardiac surgery, Clin. J. Am. Soc. Nephrol. 14 (10) (2019) 1450–1457, https://doi.org/10.2215/cjn.00690119.

[6] M.A. Brock, J.A. Coppola, J. Reid, D. Moguillansky, Atrial fibrillation in adults with congenital heart disease following cardiac surgery in a single center: analysis of incidence and risk factors, Congenit. Heart Dis. 14 (6) (2019) 924–930, https://doi.org/10.1111/chd.12857.

[7] D. Giri, D. Rigden, M. Didi, M. Peak, P. McNamara, S. Senniappan, Novel compound heterozygous ASXL3 mutation causing Bainbridge-ropers like syndrome and primary IGF1 deficiency, Int. J. Pediatr. Endocrinol. 2017 (2017) 8, https://doi.org/10.1186/s13633-017-0047-9.

[8] N. Duployez, J.B. Micol, N. Boissel, A. Petit, S. Geffroy, M. Bucci, H. Lapillonne, A. Renneville, G. Leverger, N. Ifrah, H. Dombret, O. Abdel-Wahab, E. Jourdan, C. Preudhomme, Unlike ASXL1 and ASXL2 mutations, ASXL3 mutations are rare events in acute myeloid leukemia with t(8;21, Leuk. Lymphoma 57 (1) (2016) 199–200, https://doi.org/10.3109/10428194.2015.1037754.

[9] M. Wayhelova, J. Oppelt, J. Smetana, E. Hladilkova, H. Filkova, E. Makaturova, P. Nikolova, R. Beharka, R. Gaillyova, P. Kuglik, Novel de novo frameshift variant in the ASXL3 gene in a child with microcephaly and global developmental delay, Mol. Med. Rep. 20 (1) (2019) 505–512, https://doi.org/10.3892/mmr.2019.10303.

[10] S. Zhang, F. Fu, L. Zhen, R. Li, C. Liao, Alteration of long non-coding RNAs and mRNAs expression profiles by compound heterozygous ASXL3 mutations in the mouse brain, Bioengineered 12 (1) (2021) 6935–6951, https://doi.org/10.1080/21655979.2021.1974811.

[11] F. Fu, R. Li, T.Y. Lei, D. Wang, X. Yang, J. Han, M. Pan, L. Zhen, J. Li, F.T. Li, X. Y. Jing, D.Z. Li, C. Liao, Compound heterozygous mutation of the ASXL3 gene causes autosomal recessive congenital heart disease, Hum. Genet. 140 (2) (2021) 333–348, https://doi.org/10.1007/s00439-020-02200-z.

[12] W. Xu, Q. Wu, A. Huang, Emerging role of LncRNAs in autoimmune, Lupus, Inflammation. 45 (3) (2022) 937–948, https://doi.org/10.1007/s10753-021-01607-8.

[13] Z.A. Kichi, M. Soltani, M. Rezaei, Z. Shirvani-Farsani, M. Rojhannezhad, The emerging role of EMT-related lncRNAs in therapy resistance and their applications as biomarkers, Curr. Med. Chem. 29 (26) (2022) 4574–4601, https://doi.org/10.2174/0929867329666220329203032.

[14] V. Nociti, M. Santoro, What do we know about the role of lncRNAs in multiple sclerosis? Neural Regen Res 16 (9) (2021) 1715–1722, https://doi.org/10.4103/1673-5374.306061.

[15] H.M. Okuyan, M.A. Begen, LncRNAs in osteoarthritis, Clin. Chim. Acta 532 (2022) 145–163, https://doi.org/10.1016/j.cca.2022.05.030.

[16] W.C. Ye, S.F. Huang, L.J. Hou, H.J. Long, K. Yin, C.Y. Hu, G.J. Zhao, Potential therapeutic targeting of lncRNAs in cholesterol homeostasis, Front Cardiovasc Med 8 (2021), 688546, https://doi.org/10.3389/fcvm.2021.688546.

[17] A. Shefler, M.T. Patrick, R. Wasikowski, J. Chen, M.K. Sarkar, J.E. Gudjonsson, L. C. Tsoi, Skin-expressing lncRNAs in inflammatory responses, Front. Genet. 13 (2022), 835740, https://doi.org/10.3389/fgene.2022.835740.

[18] A. Marguerie, F. Bajolle, S. Zaffran, N.A. Brown, C. Dickson, M.E. Buckingham, R. G. Kelly, Congenital heart defects in Fgfr2-IIIb and Fgf10 mutant mice, Cardiovasc. Res. 71 (1) (2006) 50–60, https://doi.org/10.1016/j.cardiores.2006.03.021.

[19] C. Huang, R. Wang, J. Lu, Y. He, Y. Wu, W. Ma, J. Xu, Z. Wu, Z. Feng, M. Wu, MicroRNA-338-3p as a therapeutic target in cardiac fibrosis through FGFR2 suppression, J. Clin. Lab. Anal. 36 (8) (2022), e24584, https://doi.org/10.1002/jcla.24584.

[20] F.E. Mundhofir, E.A. Sistermans, S.M. Faradz, B.C. Hamel, p.Ser252Trp and p. Pro253Arg mutations in FGFR2 gene causing Apert syndrome: the first clinical and molecular report of Indonesian patients, Singap. Med. J. 54 (3) (2013) e72–e75, https://doi.org/10.11622/smedj.2013055.

[21] T. Ali, P. Grote, Beyond the RNA-dependent function of LncRNA genes, Elife 9 (2020), e60583, https://doi.org/10.7554/eLife.60583.

[22] S. Panni, R.C. Lovering, P. Porras, S. Orchard, Non-coding RNA regulatory networks, Biochim Biophys Acta Gene Regul Mech 1863 (6) (2020), 194417, https://doi.org/10.1016/j.bbagrm.2019.194417.

[23] L.S. Toni, F. Hailu, C.C. Sucharov, Dysregulated micro-RNAs and long noncoding RNAs in cardiac development and pediatric heart failure, Am. J. Physiol. Heart Circ. Physiol. 318 (5) (2020) H1308–h1315, https://doi.org/10.1152/ajpheart.00511.2019.

[24] M. Touma, X. Kang, Y. Zhao, A.A. Cass, F. Gao, R. Biniwale, G. Coppola, X. Xiao, B. Reemtsen, Y. Wang, Decoding the long noncoding RNA during cardiac maturation: a roadmap for functional discovery, Circ Cardiovasc Genet 9 (5) (2016) 395–407, https://doi.org/10.1161/circgenetics.115.001363.

[25] N.J. Kim, K.H. Lee, Y. Son, A.R. Nam, E.H. Moon, J.H. Pyun, J. Park, J.S. Kang, Y. J. Lee, J.Y. Cho, Spatiotemporal expression of long noncoding RNA Moshe modulates heart cell lineage commitment, RNA Biol. 18 (sup2) (2021) 640–654, https://doi.org/10.1080/15476286.2021.1976549.

[26] J. Ma, S. Chen, L. Hao, W. Sheng, W. Chen, X. Ma, B. Zhang, D. Ma, G. Huang, Long non-coding RNA SAP30-2:1 is downregulated in congenital heart disease and

regulates cell proliferation by targeting HAND2, Front. Med. 15 (1) (2021) 91–100, https://doi.org/10.1007/s11684-020-0778-5.

[27] G. Lu, Z. Cheng, S. Wang, X. Chen, X. Zhu, Z. Ge, B. Wang, J. Sun, J. Hu, J. Xuan, Knockdown of long noncoding RNA SNHG14 protects H9c2 cells against hypoxia-induced injury by modulating miR-25-3p/KLF4 Axis in vitro, J. Cardiovasc. Pharmacol. 77 (3) (2021) 334–342, https://doi.org/10.1097/fjc.0000000000000965.

[28] Y. Zhu, Z. Feng, Z. Jian, Y. Xiao, Long noncoding RNA TUG1 promotes cardiac fibroblast transformation to myofibroblasts via miR-29c in chronic hypoxia, Mol. Med. Rep. 18 (3) (2018) 3451–3460, https://doi.org/10.3892/mmr.2018.9327.